Influence of Chain Stiffness on the Segmental Dynamics and Mechanical Properties of Cross-Linked Polymers

Xiangrui Zheng[1,2], Wenjian Nie[3], Yafang Guo[2], Jack F. Douglas[4*] and Wenjie Xia[3,5*]*

[1.] *Department of Mechanics, School of Aerospace Engineering, Huazhong University of Science and Technology, Wuhan, 430074, China*

[2.] *Department of Mechanics, School of Physical Science and Engineering, Beijing Jiaotong University, Beijing, 100044, China*

[3.] *Department of Civil, Construction and Environmental Engineering, North Dakota State University, Fargo, North Dakota 58108, United States*

[4.] *Materials Science and Engineering Division, National Institute of Standards and Technology, Gaithersburg, Maryland 20899, United States*

[5.] *Department of Aerospace Engineering, Iowa State University, Ames, Iowa 50011, United States*

[*]Corresponding authors: wxia@iastate.edu (Wenjie Xia);

jack.douglas@nist.gov (Jack F. Douglas); yfguo@bjtu.edu.cn (Yafang Guo)

Abstract

We extend previous systematic investigations of a family of model coarse-grained polymer network-forming materials by focusing on the influence of varying molecular rigidity on basic conformational properties (*e.g.*, radius of gyration R_g and persistence length l_p), segmental dynamics (structural relaxation time τ_α), and mechanical properties (shear G and bulk B moduli) of this broad class of materials. We find that increasing molecular rigidity increases the radius of gyration R_g and persistence length l_p of network chains, as observed before in polymer solutions. The increase of molecular rigidity leads to significant slowing down in the segmental dynamics and a strong increase in the characteristic temperatures (*e.g.*, onset temperature T_A, glass transition temperature T_g, and Vogel temperature T_0) and fragility of glass formation. We also find that the structural relaxation time τ_α, along with G and B, do not exhibit the near universal scaling with reduced temperature T / T_g found previously for fully flexible cross-linked networks having variable cross-link density and cohesive energy but a *fixed* bending stiffness. Both of these moduli become progressively *smaller* in magnitude as the network chains get stiffer over the T range investigated. Moreover, τ_α and the moduli (G, B) all exhibit strong correlative relationships with the Debye-Waller parameter $<u^2>$, which is correspondingly utilized to define a *local* measure of material "stiffness". Color maps based on this stiffness measure indicate that both the average value and variance of the local stiffness fluctuations decrease with an increasing chain stiffness at the same reduced temperature, T / T_g. Our simulation observations provide novel physical insights into how varying chain stiffness influences glass formation of cross-linked networks that should be helpful in the design of cross-linked thermoset materials.

1. Introduction

Cross-linked polymer materials and thermoset materials, in particular, are widely used in structural, engineering, and biomedical applications due to their superior mechanical properties, excellent chemical resistance, and heat stability. Upon cooling down towards their glass transition temperatures T_g, polymer melts characteristically exhibit a pronounced slowing down in relaxation dynamics and a strengthening in mechanical properties, and this is also a conspicuous property of thermoset polymer materials.[1] Numerous experimental and simulation studies have demonstrated that various molecular factors, such as chemical structure,[2,3] cross-link density,[4,5] chain stiffness[6,7] and additives,[8,9] all can have a significant influence on the dynamics and mechanical properties of polymer materials. Our investigation is premised on the idea that a clear understanding of the influence of a minimal set of molecular parameters on glass formation in coarse-grained models of polymer network materials, should be helpful in identifying general trends in the relaxation and mechanical properties of these model materials that can be utilized in improving the performance and rational design of real polymer network materials.

Experimental and computational studies on polymer materials have repeatedly established that chain stiffness is a primary molecular variable governing segmental relaxation dynamics and diffusion processes in polymer materials broadly, and it is generally appreciated that this molecular parameter can also greatly impact the mechanical properties of polymer materials. Polymers with rigid or sterically hindered backbones usually exhibit broad segmental dispersions and steep temperature dependence of segmental relaxation.[2,10] Sokolov *et al.*[11,12] performed a series of experiments to explore the relationship between ionic conductivity and structural relaxation in

polymer electrolytes using dielectric spectroscopy, where the polymer with rigid backbones exhibited significant packing frustration and strong decoupling of ion diffusion from structural relaxation. Subsequently, this experimental observation was also confirmed by the coarse-grained (CG) molecular dynamics (MD) simulation.[13] Lesser and coworkers[14,15] performed a series of mechanical and thermodynamic measurements on epoxy resins, where the chain stiffness was found to exhibit a significant influence on the primary relaxation and yield strength, but had only a negligible effect on the glassy moduli. Surface wrinkling and spectroscopic ellipsometry experiments in poly[5-(2-phenylethylnorbornene)] derivatives demonstrated that T_g and the shear elastic modulus were independent of film thickness for thin films with stiff backbones, whereas they decreased with thickness when the backbones of polymers were relatively flexible.[6] Chain stiffness is usually varied by changing the chemical structure of polymers in experiments, but varying chemical structure can also lead to changes in the cohesive interaction strength, so that it is difficult to study the effect of chain rigidity on glass formation in complete isolation from other molecular variables impacting glass formation.[6,14] One of the advantages of simulation is that it allows for the variation of chain stiffness in isolation from other effects.

Various simulation works on the polymer materials have indicated that the chain stiffness has an important effect on the chain conformation and morphology,[16–19] relaxation dynamics,[13,20–24] and mechanical properties.[7,16,24] Previous studies of pure and nanocomposite polymer materials have indicated a general slowing of the rate of relaxation dynamics with increasing chain stiffness and a higher fragility of glass formation,[13,21,22] effects attributed to an increase in packing frustration. Subsequently, Lu *et al.*[21] explored the role of side-chain stiffness in the relaxation

dynamics of free-standing films, where it was found that polymers with stiffer side-groups exhibited a higher fragility. Xu *et al.*[25] explored the influence of relative rigidities of backbones and side-chains on glass formation for branched polymers using CG-MD simulations and generalized entropy theory (GET).[26] They observed that both T_g and fragility decreased with the increasing side-chain length for branched polymers with stiff backbone and flexible side chains, while the opposing trend was observed in polymer melts with flexible backbone and stiff side-chains. In addition, CG-MD simulations performed by Ness *et al.*[7] on the mechanical response of glassy linear polymers indicated that the storage modulus exhibited a nonmonotonic variation with the increase in chain stiffness, which could be ascribed to the competing effects between the increasing chain rigidity and increasing "free volume".

Most previous simulation studies of glass formation in polymer materials have been based on uncross-linked polymers and polymer composites, and many aspects of the segmental relaxation dynamics and mechanical properties of cross-linked thermoset materials are still unknown. Dielectric spectroscopy experiments performed by Rolla *et al.*[27,28] have shown that the progressive introduction of cross-links at constant temperature can lead to chemical vitrification of epoxy resins. And the effect of cross-link density on glass formation has been widely studied recently for a range of cross-linked polymer materials,[4,5,27–32] where the structural relaxation time and T_g, along with the fragility of glass formation and dynamical heterogeneity all have been found to increase significantly during the network "curing" process. Similar trends in dynamical properties have also been observed in star and ring polymers with the increasing topological complexity,[33–36] which indicates that polymer topology can also greatly influence glass formation of polymer materials.

There are evidently a number of contributing effects influencing the segmental dynamics when the molecular topology is altered in real materials. In particular, changes in molecular topology can significantly alter average molecular shape and size both in the melt and in solution,[33,34,37,38] and large changes in topological complexity can induce appreciable changes in the persistence length.[33,34] Since changes in molecular packing must generally lead to changes of cohesive interaction strength, significant changes in molecular topology cannot be made completely independently from changes of the effective cohesive interaction strength and molecular rigidity. These central molecular variables for polymer glass formation are in general *coupled* in their effect on glass formation.

Mei *et al.*[30] investigated the segmental dynamics of semi-flexible polymer networks with varying cross-link density, where excellent agreement was claimed among broadband dielectric spectroscopy experiments, CG-MD simulation and elastically collective nonlinear Langevin equation (ECNLE) theory. Elder *et al.*[31,39,40] performed a series of atomistic MD simulations to explore the relaxation dynamics and mechanical properties based on the cross-linked poly(dicyclopentadiene) networks, where the atomistic mobility was found to become progressively more heterogenous due to the introduction of polar functionality to the polymers, a molecular parameter that can greatly influence the cohesive interaction between the molecules. In our previous work,[41,42] we explored in isolation the effect of cross-link density and cohesive energy on the relaxation dynamics and mechanical properties for cross-linked polymer networks using CG-MD simulation, which agreed well with the experiments,[14,15,32] simulations[30,39,43,44] and GET.[26,45] However, the polymer chains used in our previous work were assumed to be ideally

flexible.

A series of CG-MD simulations combined with GET performed by Xu *et al.*[23,46,47] demonstrated that the bending constraints played a critical role in the thermodynamics and dynamical properties of linear polymer melts, where the characteristic temperatures and fragility of glass formation exhibited different variation trends with the increasing cohesive energy for polymer melts with and without bending constraints.[43,46,47] We may then anticipate that changing polymer rigidity should likewise lead to appreciable changes in the thermoset dynamical properties, although it is not all clear that changing the polymer rigidity in thermosets should have the same effect as found in linear polymer melts. In the present work, we continue our systematic study of model cross-linked polymer materials to explore the influence of varying chain stiffness on basic conformational properties, dynamical and mechanical properties for our model coarse-grained thermoset material over a wide range of temperatures (T) where the cohesive interaction strength and cross-link density are fixed. We hope the findings of the present work will contribute to building a basic conceptual framework for understanding what molecular parameters are most relevant to understanding and controlling the segmental dynamics of cross-linked polymers.

2. Model and Simulation Details

2.1. Coarse-Grained (CG) Model. The cross-linked polymers are represented by the bead-spring model in this paper,[48] which is widely used to study the glass formation of polymers.[5,44] The CG model of cross-linked polymers is composed of 1200 linear chains with each consisting of ten beads and 600 tetra-functional cross-linkers with star structure. Every cross-linker

contains a core and four arms with one bead in each arm (**Figure 1a**). It is notable that the "cartoon" illustration of molecular structures in **Figure 1** only describes the initial geometry structures, but not their actual configurations exhibited in the cross-linked thermosets. The linear chains and cross-linkers are initially mixed in a large cubic simulation box with periodic boundary conditions in all directions.

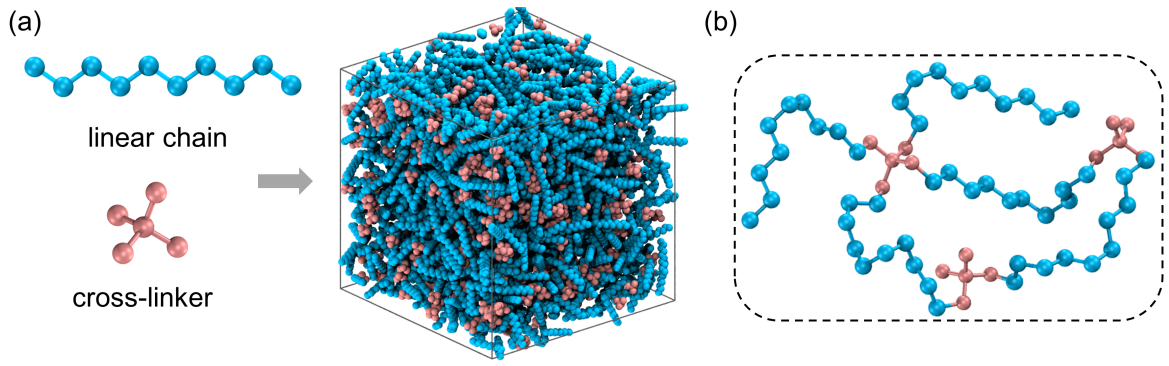

Figure 1. (a) A "cartoon" illustration describing initial molecular geometry structures of linear chain (blue beads) and cross-linker (pink beads), which do not represent their actual configurations exhibited in the cross-linked polymers. (b) Schematic of polymer network structure. The cross-link density is defined as the percentage of reacted end beads of cross-linkers in the total number of end beads of cross-linkers. For example, there are three cross-linkers and thus twelve reactive end beads, where eight end beads have been bonded with linear chains while four active beads are not yet reacted. Hence, the cross-link density is regarded as the ratio of eight to twelve, *i.e.*, 75 %.

The non-bonded interactions are represented by the standard truncated and shifted Lennard-Jones (LJ) potential,

$$U_{\mathrm{LJ}}(r)=\begin{cases}4\varepsilon\left[\left(\dfrac{\sigma}{r}\right)^{12}-\left(\dfrac{\sigma}{r}\right)^{6}-\left(\dfrac{\sigma}{r_{\mathrm{c}}}\right)^{12}+\left(\dfrac{\sigma}{r_{\mathrm{c}}}\right)^{6}\right], & r<r_{\mathrm{c}}\\ 0, & r\geq r_{\mathrm{c}}\end{cases} \tag{1}$$

where r is the distance between two beads, $r_c = 2.5\ \sigma$ is the cutoff distance, σ governs the effective van der Waals radius, and ε describes the cohesive energy strength of the cross-linked polymers. The bond connectivity along neighboring beads is determined via the finitely extensible nonlinear elastic (FENE) potential,

$$U_{\mathrm{FENE}} = -0.5KR_0^2 \ln\left[1-\left(\frac{r}{R_0}\right)^2\right] + 4\varepsilon\left[\left(\frac{\sigma}{r}\right)^{12} - \left(\frac{\sigma}{r}\right)^{6}\right] + \varepsilon \quad (2)$$

where the force strength $K = 30\ \varepsilon/\sigma^2$ and the maximum bond length $R_0 = 1.5\ \sigma$. The first term is attractive and the second LJ term is repulsive with a smaller cutoff distance $R_c = 2^{1/6}\ \sigma$. The bending constraint is modeled by a simple cosine angular potential,[49,50]

$$U_{\mathrm{bend}}(\theta) = k_\theta\left[1+\cos(\theta)\right] \quad (3)$$

where k_θ describes the bending strength, θ is the angle composed of three consecutive bonded particles. To explore the influence of chain stiffness on the glass formation of cross-linked polymers, we systematically vary the chain stiffness parameter k_θ of linear chains (blue beads in the **Figure 1**) from 0.0 ε to 2.0 ε. The k_θ of cross-linkers (pink beads in the **Figure 1**) is fixed at 1.0 ε, while the molecular stiffness parameter k_θ of bond angles formed between the linear chains and cross-linkers is determined as the average value of linear chains and cross-linkers. Everaers *et al.*[51] recently tuned the chain stiffness of a Kremer-Grest polymer model to match the real polymers based on the number of Kuhn segments per Kuhn volume, where they found that the Kremer-Grest model with chain stiffness in a range of 0.0 ε to 2.0 ε could map a wide range of polymers from a flexible polydimethylsiloxane to a stiff polyethylene. All the quantities are expressed in the standard reduced LJ unit for convenience. The basic quantities, length σ, energy ε and mass of each

bead m, are set to be unity. Other units of interest can be derived from these fundamental units. For example, time τ, temperature T and pressure P can be described in units of $\tau_{LJ} = (m\sigma^2/\varepsilon)^{1/2}$, ε /k_B and ε /σ^3, respectively.

2.2. Simulation Details. We briefly describe the simulation method here, which has been described in detail in our preceding works focusing on the same cross-linked polymer model.[41,42] All the MD simulations are performed in Large Scale Atomic/Molecular Massively Parallel Simulator (LAMMPS) software.[52] The mixture of linear chain and cross-linkers are relaxed in a constant pressure and constant temperature (NPT) ensemble for $t = 2 \times 10^4$ τ_{LJ} at a temperature $T = 2.0$ ε /k_B and a pressure $P = 0.0$ ε /σ^3, and then T is decreased to $T = 1.0$ ε /k_B over a period of $t = 2 \times 10^4$ τ_{LJ}, followed by a canonical (NVT) relaxation for a period of $t = 1 \times 10^4$ τ_{LJ}, to ensure that the linear chains and cross-linkers are homogenously mixed. A cross-linking algorithm proposed by Varshney *et al.*[53] is utilized to cross-link the molecules into a three-dimensional network, which has successfully captured the thermodynamics and mechanical properties of various cross-linked polymer networks.[53–55] In particular, the two end beads of each linear chain and four end beads of each cross-linker are set as the reactive beads, which have the ability to form new bonds. When the distance between an end bead of linear chain and an end bead of cross-linker is less than 1.3 σ, a new bond is created between the two beads. Then an NPT relaxation process is subsequently preformed to equilibrate the new cross-linked structure. Based on the new cross-linked structure, a next iteration of cross-linking is started. The cross-linking algorithm is finished until the percentage of reacted end beads of cross-linkers in the total number of end beads of cross-linkers (defined as cross-link density next) is over 90 %. The cross-link

density of the final cross-linked network is 93.75 %. We emphasize here that the simulation results reported in the present work is only based on one cross-link density. The influence of cross-link density on the glass formation of cross-linked thermosets with bending constraints deserves to study further.

To explore the isolated effect of chain stiffness on the glass formation of cross-linked polymer networks, five systems with the same cross-linked structure but different linear chain stiffness are produced. First, the five systems are relaxed in the NPT ensemble over a period of $t = 3 \times 10^4\ \tau_{LJ}$ at $T = 2.0\ \varepsilon / k_B$. Then, the relaxed systems are quenched from a high temperature $T = 2.0\ \varepsilon / k_B$ to a low temperature $T = 0.1\ \varepsilon / k_B$ in a stepwise fashion with a temperature step size of $\Delta T = 0.05\ \varepsilon / k_B$. At each temperature, the systems are relaxed in an NPT ensemble for $t = 2 \times 10^4\ \tau_{LJ}$ and in an NVT relaxation for $t = 1 \times 10^4\ \tau_{LJ}$, then the configurations are collected at the end of each run. The system with different chain stiffness is denoted as k_θ = x, which means that the chain stiffness parameter of linear chains is x in the corresponding cross-linked polymer model.

3. Results and Discussion

3.1. Conformational Properties. Considering the established influence of chain stiffness on the conformational properties of linear polymer melts,[18,56] we first analyze the thermodynamic properties (Figure S1 in the Supporting Information) and conformation of cross-linked polymers with a wide range of chain stiffness. In particular, the thermodynamic properties (*e.g.*, number density ρ, reduced thermal expansion coefficient α_p^*, reduced isothermal compressibility κ_T^* and static structure factor $S(q)$) are found to be insensitive to the variation of

chain stiffness, as observed in linear polymer melts with varying chain rigidity and predicted by GET.[46]

Figure 2a shows the radius of gyration R_g and end-to-end distance R_e of network chains as a function of chain rigidity k_θ where the cross-link density, temperature and the cohesive interaction strength are all held fixed. As expected, the R_g and R_e increase with increasing chain stiffness, which agreed well with the widely observed trend in semi-flexible linear polymer melts as the chain stiffness increased.[16–18,22] In addition, we also estimate the persistence length l_p of network chains with varying chain stiffness using the autocorrelation function, $C(s) = \langle \boldsymbol{b}_s \cdot \boldsymbol{b}_0 \rangle$, where $\boldsymbol{b}_s$ is the unit vector aligned along the $(s + 1)^{th}$ bond along the network chains, and $\boldsymbol{b}_0$ is the first bond in the chain. In this work, the persistence length l_p is defined as the characteristic length when the $C(s)$ decays to 0.2, regardless of whether the decay is exponential as predicted by the ideal worm-like chain model or not.[33,34] As shown in **Figure 2b**, we find that the l_p increases when the cross-linked network gets rigid, which is consistent with the trend found in the semi-flexible linear polymer melts.[49] Narambuena *et al.*[18] systematically investigated the role of chain stiffness played in the morphology of polyelectrolyte complexes using Monte Carlo simulation, where they found that the structure of polyelectrolyte complex gradually changed from a globular shape to a pseudo-toroidal shape, and finally stretched to a rigid rod when the polyanion linear chains became sufficiently stiff. Along with the changes in the morphology, the end-to-end distance, radius of gyration and persistence length of polyanion chains all became larger with the increase in chain stiffness.

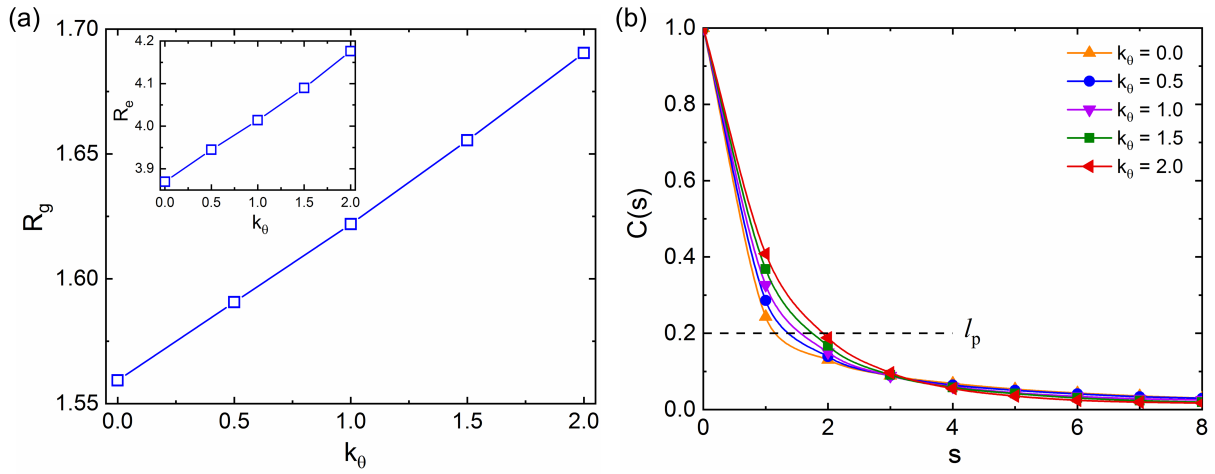

Figure 2. The conformational properties of network chains at $T = 2.0\ \varepsilon / k_B$ as a function of the chain stiffness parameter, k_θ. (a) Network chain radius of gyration, R_g. The inset describes the end-to-end distance, R_e. (b) Determination of persistence length, l_p.

3.2. Structural Relaxation Dynamics. We analyze the effect of chain stiffness on the structural relaxation dynamics from the structural relaxation time τ_α, which is a central quantity in the glass formation. The τ_α is determined from the self-part of the intermediate scattering function $F_s(q, t)$,

$$F_s(q,t) = \frac{1}{N}\left\langle \sum_{j=1}^{N} \exp\left\{-i\boldsymbol{q}\cdot\left[\boldsymbol{r}_j(t) - \boldsymbol{r}_j(0)\right]\right\}\right\rangle \tag{4}$$

where the wavenumber $q = |\boldsymbol{q}|$ is chosen to be 7.1 σ^{-1} in our cross-linked polymer network models, close to the first peak of the static structure factor (Figure S1d in the Supporting Information).[41] $\boldsymbol{r}_j(t)$ is the coordinate of particle j at time t, and $\langle\cdots\rangle$ indicates that $F_s(q, t)$ is averaged over all beads and over distinct initial times. The τ_α is defined as the time when $F_s(q, t)$ decays to 0.2.[33,46,57] In order to reduce errors in the estimation of τ_α, a timestep of 0.002 τ_{LJ} or 0.01 τ_{LJ} is utilized in the high or low T, respectively. We plot the $F_s(q, t)$ curves at a higher temperature $T = 1.0\ \varepsilon / k_B$ and a

lower temperature $T = 0.55\ \varepsilon\ /k_B$ in the Figure S2a in the Supporting Information. The $F_s(q, t)$ exhibits a two-step decay, consisting of a "fast β-relaxation" on the ps timescale and an α-relaxation which normally occurs on a much longer timescale. These relaxation processes has been widely observed and quantified in various metallic and polymeric glass-forming materials,[13,41,46,58] and this kind of two-step relaxation process is apparently a universal property of glass-forming liquids. It is notable that the $F_s(q, t)$ curves for cross-linked thermosets with a wide range of chain stiffness nearly collapse onto a universal curve at a high temperature $T = 1.0\ \varepsilon\ /k_B$, indicating a weak influence on the fast β-relaxation and α-relaxation. While at a low temperature $T = 0.55\ \varepsilon\ /k_B$, the $F_s(q, t)$ curves exhibit an obvious difference in the α-relaxation time. A specific two-step relaxation function has been found to successfully describe simulation observations of $F_s(q, t)$ for a variety of glass-forming materials,[41,42,58,59]

$$F_s(q,t) = (1 - A_\alpha) e^{-(t/\tau_f)^{\beta_f}} + A_\alpha e^{-(t/\tau_\alpha)^{\beta}} \quad (5)$$

where the prefactors A_α and $1 - A_\alpha$ are the relative strength of α- and fast β-relaxation processes having relaxation times τ_α and τ_f, respectively, and the exponents β and β_f describe the deviation of these relaxation processes from an exponential decay. The fitting parameters τ_f and β_f have been found to be insensitive to T in previous studies of metallic and polymeric glass formers when the T is varied over a moderate range.[41,42,58,60] And thus, we estimate the τ_f, β_f and β over a wide range of T for cross-linked networks with varying chain stiffness in Figure S2 in the Supporting Information, where all of them seem to be weakly dependent on chain stiffness at higher temperatures, consistent with a similar $F_s(q, t)$ curve for cross-linked thermosets with varying chain stiffness at a high temperature $T = 1.0\ \varepsilon\ /k_B$. In particular, τ_f is found to increase upon cooling,

consistent with the trend observed in τ_α. The exponent parameters β_f and β are found to slightly increase with elevating T, and a similar increasing trend was observed by Giuntoli *et al*. in the CG polymer melt model.[59]

As a characteristic of glass-forming polymer liquids, we see in **Figure 3a** that τ_α increases significantly upon cooling at fixed stiffness. The progressive introduction of bending constraints results in a much longer τ_α at a fixed lower T, while the effect of changing chain stiffness on τ_α is relatively weak at high T, again as normally observed in linear polymer melts.[13,46,50] In many ways, the relaxation dynamics of our thermoset materials resemble most any other molecular glass-forming liquids. At high temperatures, there is a "simple fluid" regime in which τ_α follows an Arrhenius T-dependence, and then a non-Arrhenius T-dependence sets in below the onset temperature T_A. This transition between the high-T Arrhenius regime and a low-T non-Arrhenius regime was discussed at length in the review by Xu and coworkers.[45] In general, the activation enthalpy can depend appreciably on the intermolecular interaction strength, pressure, molecular topology, *etc*., but the dependence of the activation enthalpy on stiffness would appear to be rather weak in our model. In the molecular dynamic simulations,[36,40,46] a wide temperature range is usually considered to observe the entire process of glass formation rather than just a temperature near the calorimetric glass transition. It is perhaps worth noting that that most polymers start to thermally degrade before reaching this high-T regime so that the Arrhenius regime is normally physically inaccessible in polymers. Thus, we emphasize that the Arrhenius regime at a very high T is only limited in our cross-linked thermosets model with a fixed cross-link density and cohesive energy, which deserves to confirm further in the experiments.

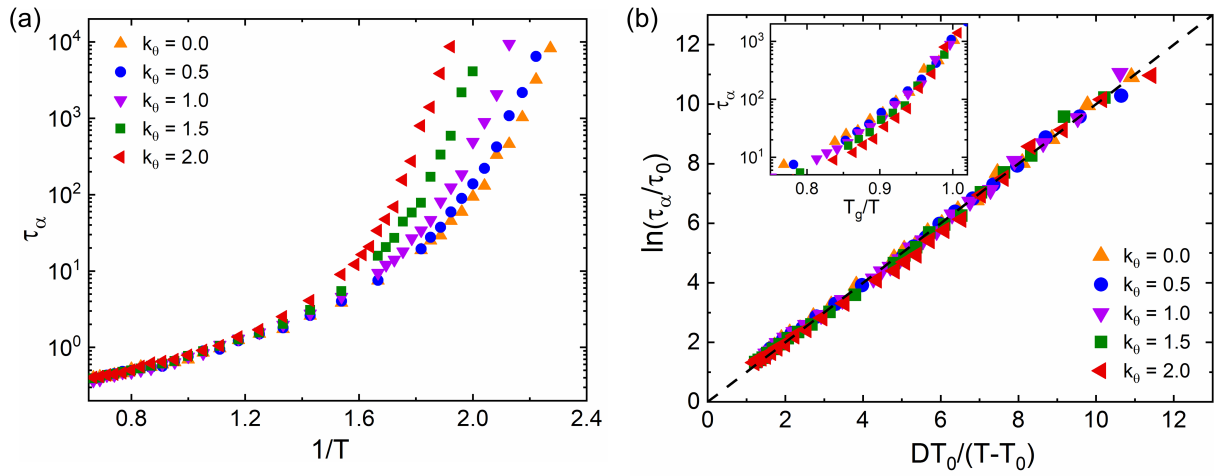

Figure 3. (a) The structural relaxation time τ_α as a function of $1 / T$ for cross-linked networks with varying chain stiffness k_θ. τ_α increases significantly with the increasing k_θ at lower T. (b) The VFT collapse of T-dependence of τ_α for various k_θ. Dashed line indicates the VFT relation, $\ln(\tau_\alpha / \tau_0) = D\, T_0 / (T - T_0)$. The good collapse onto the dashed line indicates that the VFT equation can describe the relaxation dynamics well for cross-linked networks with varying k_θ. The inset descripts the structural relaxation time τ_α as a function of reduced temperature T_g / T. This lack of reduction implies that τ_α is not a universal function of T_g / T. The origin of this lack of scaling is described in the text.

Numerous simulation works and experimental studies on polymer glass formation[5,33,61] have shown that the Vogel-Fulcher-Tammann (VFT) relationship, $\tau_\alpha = \tau_0 \exp[D\, T_0 / (T - T_0)]$, provides a good empirical description of τ_α over a wide range of temperatures below T_A but above the glass transition temperature T_g. As a "reality check", we fit our τ_α data for cross-linked polymer networks having a wide range of k_θ to the VFT equation (**Figure 3b**), and as usual we find a good collapse of all our data. We have seen such agreement before in previous coarse-grained simulations of fully flexible and semi-flexible linear polymer melts,[13,46,47] single-chain cross-linked nanoparticle melts,[5] poly(methyl methacrylate) bulk polymers and supported thin films[57] and conjugated

poly(3-hexylthiophene) melts.[61] Our relaxation data conform to the standard phenomenology of glass formation, and we are then in position to explore how the chain stiffness of our thermoset model alters the fragility ($K \equiv 1 / D$), T_g, and the mechanical properties (G, B) of this class of materials.

The generalized entropy theory (GET),[26,45,62] which combines the lattice cluster theory[63] with Adam-Gibbs (AG) model,[64] has successfully predicted general trends in how molecular structure and thermodynamical conditions influence segmental relaxation behaviors of polymer melts.[25,47,57] This theory provides some guidance on what properties would be interesting to calculate and some expected trends, even though the theory has not yet been developed to describe branched polymer networks because of the technical complexity of such calculations. For example, the GET indicates that glass formation involves a broad thermodynamic transition (not a phase transition) exhibiting multiple characteristic temperatures,[26,62] and these characteristic temperatures are strongly dependent on molecular factors, such as cohesive energy[43] and chain stiffness.[46,62] The VFT equation can be derived from the GET over the restricted T range in which this phenomenology is observed, where the parameters of this equation are further specified in terms of parameters determined through comparing the GET to experiments on thermodynamic properties. Xu *et al.*[43,46,47] performed CG-MD simulations on model glass-forming linear polymer melts in conjunction with the GET calculations, and found that both approaches to model polymer materials indicated that all the characteristic temperatures of glass formation (defined and estimated by CG-MD simulation below for thermoset polymers) increased linearly with the cohesive energy for fully flexible polymer melts, while they exhibited a non-linear variation with the cohesive energy

for polymer melts subjected to bending constraints. Considering the important role that bending constraints play in altering the characteristic temperatures of glass formation in linear polymers, we next explore the effect of chain stiffness on the characteristic temperatures for cross-linked polymer networks below (**Figure 4a**) following a by now standard computational methodology.

As seen in **Figure 3a**, τ_α exhibits a high-T Arrhenius regime, $\tau_\alpha = \tau_\infty \exp(\Delta E / k_B T)$, and we define the "onset temperature" T_A by the condition at which τ_α departs from the high-T Arrhenius relation by an amount larger than 1 %, *i.e.*, $[\tau_\alpha - \tau_\alpha(\text{Arrhenius})] / \tau_\alpha > 10^{-2}$,[41–43] where τ_α(Arrhenius) is the expected structural relaxation time from Arrhenius fitting. We see a nearly linear increase in T_A with k_θ, similar to the trend observed in the linear polymer melts and their thin films where the rigid linear polymer exhibited a higher T_A.[49] Next, T_g is estimated from the VFT equation using a similar range of τ_α for cross-linked polymer networks with varying k_θ. The upper bounds for T are taken to be T_A, and the lower bounds are just the lowest T available in our simulations. In order to reduce the uncertainty in the long extrapolation of the VFT relation to estimate T_g, a "computational" T_g[24,35,57,65] is used in this work based on the definition of $\tau_\alpha(T_g) = 10^3\ \tau_{LJ}$. The "computational" T_g corresponds to a laboratory timescale on the order of 1 ns, which has been found to accord well with that estimated from the thermodynamic criterion[35,41] and that estimated from the common empirical definition of $\tau_\alpha(T_g) = 100$ s.[24,41,65] It is found that T_g increases obviously with k_θ. This trend is again consistent with previous observations in the linear polymer melts,[46,66] ionomeric polymers,[20] free-standing thin films[21] and semi-flexible polymer brushes.[19] In situ ellipsometry experiments have also indicated an increase in T_g arising from a rigidity change in the polymer induced by saturating the side-chain of the phenyl ring to form a cyclohexyl

moiety.[6] The Vogel temperature T_0, which describes the end of glass transition, exhibits a similar trend with that observed in T_g. The cross-linked networks with more rigid chains exhibit a larger T_0.[25] Compared to the linearly increasing trend exhibited in our coarse-grained cross-linked thermoset model, Xu *et al.*[46] observed a non-linear increasing trend with the chain stiffness based on a different bending potential in linear polymer melts. Thus, we emphasize that the linear trend in T_g and the other characteristic temperatures of glass formation indicated in **Figure 4a** is restricted to our model of cross-linked polymer networks under the range of chain rigidity and cross-link density considered in our study. In summary, all the characteristic temperatures increase with the chain stiffness in a parallel fashion to polymer melts with varying backbone or side-chain stiffness.[21,46,49,50] The trend observed seems to be a general nature in polymer materials.

In addition, the inset of **Figure 4a** descripts the normalized characteristic temperatures by their values at chain stiffness $k_\theta = 0.0\ \varepsilon$, where the characteristic temperatures vary in a different slope with the chain stiffness. The T_A exhibits the most sensitive dependence on the chain stiffness k_θ, while the change of T_g with k_θ is weaker. Notably, the characteristic temperature ratio (*e.g.*, T_0 / T_g, T_0 / T_A) have previously been taken as estimates of the "breadth" of glass transition and the fragility of glass formation,[46,67] where a smaller T_0 / T_g or T_0 / T_A corresponds to a stronger glass former (stronger glass-forming liquids typically have broader transitions). And thus, we further estimate the characteristic temperature ratio T_0 / T_g in the inset of **Figure 4b**, which is found to increase obviously with the increasing k_θ, consistent with the results in the inset of **Figure 4a**. The results indicate that introducing the bending constriants leads to a narrower glass transition and a more fragile glass former.[23,49,66]

Except for the characteristic temperature ratio, we also measure the kinetic fragility of glass formation determining the steepness of T-dependence of τ_α upon approaching T_g from fitting our τ_α data to the VFT equation. The "fragility parameter" $K \equiv 1 / D$ using this standard analysis is shown in **Figure 4b**. The fragility of glass formation is evidently higher for cross-linked polymer networks having stiffer chains, a trend that accords with the GET prediction for linear chains having increased chain stiffness.[26] We see in **Figure 4b** that the increase in fragility with increasing chain stiffness is relatively weak when the network chains are initially highly flexible (a small k_θ). An increase in K or decrease in D with the increasing backbone or side-chain stiffness has been widely reported in CG-MD simulations of linear polymer melts and thin polymer films,[13,21,46,49,50] where more rigid chains were found to exhibit more significant packing frustration. And the GET theory predicts that this situation should result in a more fragile glass former (provided the cohesive interaction strength is not also varied at the same time), as observed in our simulations.

Roland *et al.*[10] systematically explored the effect of chemical structure on the segmental relaxation behavior using dielectric measurements, where the structural relaxation time exhibited more sensitive T-dependence for polymers with rigid backbones or sterically hindering side-groups. The experiments performed by Kunal *et al.*[2] and Duarte *et al.*[3] over a wide range of polymer melts with varying backbone and side-chain structures indicated that the fragility was controlled by the relative flexibility of side-chains and backbones. The fragility was found to increase when either the side-chain stiffness or the backbone stiffness became larger than the other, which was confirmed in the high molar mass polymers with poly(α-pentene) structure based on the GET,[66] and in the CG-MD simulations for branched polymer melts with varying side-chain length.[25]

In addition, in our previous work on fully flexible cross-linked networks with varying cross-link density,[41] the structural relaxation time τ_α collapsed onto a master curve at the reduced temperature $(T - T_g) / T_g$, which could be well described by a modified Williams-Landel-Ferry (WLF) function. Dudowicz *et al.*[68] held that the well-known WLF scaling relationship describing the *T*-dependence of structural relaxation time in polymer materials, along with the near "universal" constants of this phenomenological equation, is a consequence of an empirical near proportionality between K and T_g in many polymer materials. Note that K does not change in the same way with k_θ as T_g when the bending constraints are introduced, so that the structural relaxation time τ_α should not be a near universal function of $(T - T_g)$ or T_g / T.[68] Thus, we estimate the τ_α as a function of T_g / T at a narrow temperature range near glass transition ($T_g < T < 1.2\ T_g$), where the WLF function is applicable. This proportionality relation evidently no longer holds in our network materials when chain stiffness is varied over a large range (inset of **Figure 3b**).

We also estimate the relaxation dynamics for uncross-linked melts with the same molecular structure and bending energy as used in the present work, and the results are shown in Figure S3 in the Supporting Information. It is no doubt that the uncross-linked melts exhibit faster relaxation dynamics than the highly cross-linked thermosets, along with a smaller T_g and fragility. The progressive introduction of cross-links again leads to a more fragile glass former, consistent well with the simulation trend observed in the fully flexible crosslinked polymers with a wide range of cross-link density,[41] and experiments results based on the polyvinylethylene networks,[4] dimethacrylate networks,[69] and cross-linked poly(methyl methacrylate) polymer.[32] We next turn to a "dynamical free volume" description of the segmental dynamics and mechanical properties of

our model thermoset materials since this approach provides complementary insights into property changes than the GET based framework.

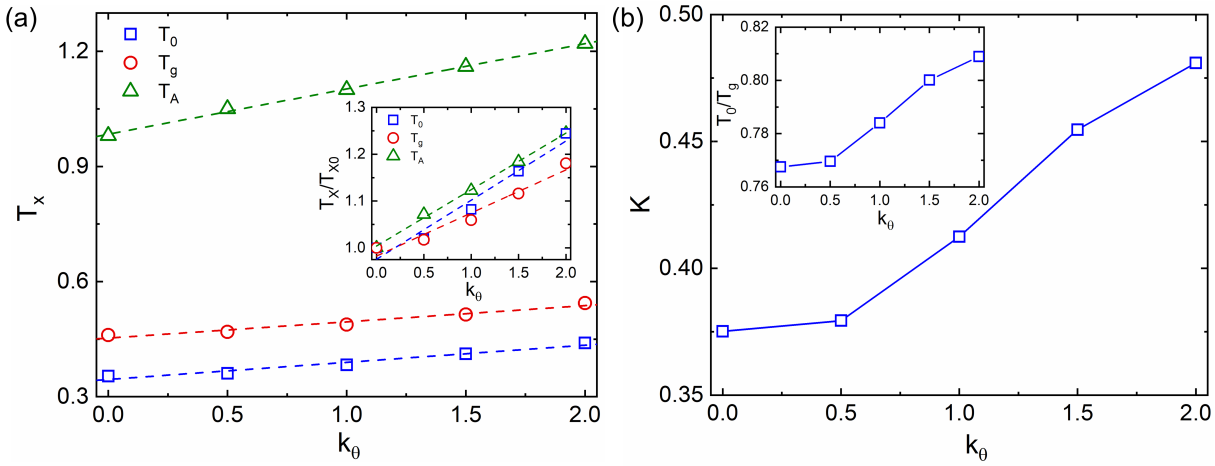

Figure 4. (a) The characteristic temperatures (*e.g.*, onset temperature T_A, glass transition temperature T_g and Vogel temperature T_0) for cross-linked polymer networks with varying chain stiffness k_θ. The inset descripts the normalized characteristic temperature by its value at $k_\theta = 0.0\ \varepsilon$. The dashed lines descript the linear fitting. (b) The fragility parameter K as a function of k_θ. The inset descripts the characteristic temperature ratio T_0 / T_g as a function of the chain stiffness parameter k_θ.

The Debye-Waller parameter $\langle u^2 \rangle$ quantifies the average "rattling amplitude" of the center of mass of polymer segments on the ps timescale over which the molecules are caged by their neighbors, and correspondingly $\langle u^2 \rangle^{3/2}$ quantifies the volume explored by the molecule, a variety of "dynamical free volume".[70] The Debye-Waller parameter should not be confused with conventional definitions of free volume based on local density, since the kinetic energy of the molecule, as well as space available for movement in conventional free volume theory, has an appreciable influence on $\langle u^2 \rangle$. Several theoretical models have been introduced to rationalize the

observed strong correlation between $\langle u^2 \rangle$ and τ_α. For instance, Leporini and coworkers[71–73] introduced a specific model to describe the relationship between τ_α and $\langle u^2 \rangle$ based on the general shoving model framework, which has been confirmed in a wide range of glass formers.[71] Simmons and co-workers[74] also proposed a generalized localization model (LM) based on the dynamical free volume perspective just mentioned. Betancourt and co-workers[75] refined the LM by reducing the number of free parameters in this model by reducing $\langle u^2 \rangle$ by its observed value at the onset temperature T_A, $u_A^2 \equiv \langle u^2(T_A) \rangle$. This simple extension in the LM led to a remarkable simple relation for the structural relaxation time,

$$\tau(T) = \tau_A \exp\left[\left(u_A^2 / \left\langle u^2(T) \right\rangle\right)^{\alpha/2} - 1\right] \tag{6}$$

where the exponent α is the only empirical parameter, which descripts the anisotropy of local dynamic free volume, and $\tau_A \equiv \tau_\alpha(T_A)$. The exponent α was found to be about 3 for a variety of glass formers, such as polymer nanocomposites with a range of concentrations and thin-films with varying thickness,[75] and polymer melts with additives having various sizes and interaction strength.[9] Whereas, Simmons *et al.*[74] argued that α should generally be variable because of the anisotropic shape of dynamical free volume regions deriving from the inherent anisotropy of intermolecular potential interactions in polymer molecules. Thus, Simmons and coworkers[76] examined the variation of this empirical exponent for a wide range of glass-forming liquids, spanning polymers, small organic molecules, inorganic and metallic glass-forming materials, and found that the LM exponent α was rather variable. Despite the empirical success of the LM, it remains in large measure phenomenological, and it is of interest to study how α varies in cross-

linked polymer networks.

Here we test the LM relationship for cross-linked polymer networks with a wide range of chain stiffness k_θ in **Figure 5**. The Debye-Waller parameter $\langle u^2 \rangle$ is precisely defined in the work as the mean-square displacement of polymer segments at $t = 1.0\ \tau_{LJ}$ (≈ 1 ps in laboratory units). As in past applications of the LM, we find a good reduction of all our relaxation data for polymer networks with different chain stiffness, where α is estimated to lie in a range between 2.4 to 2.1. Ruan and Simmons[20] found that the exponent increased from 2.62 to 3.86 with the increasing chain stiffness of ion-free homopolymers, and a little larger value was observed in the ionomeric polymers than that in the ion-free polymers. α in polymer/diluent blends[24] was reported to increase significantly with increasing diluent stiffness, and gradually plateaued at 3 when the stiffness of diluent was sufficiently large. In addition, the α was estimated to be 1.9 and increased with the cohesive interaction strength for the fully flexible networks in our previous works based on the same cross-linked network model.[42] Compared to the α value found for fully flexible networks, the larger exponent value observed in the cross-linked networks with bending constraints suggests that the introduction of chain stiffness results in a significant local anisotropy of free volume if this model is taken to correctly describe the variation of α. In general, the good fitting of the LM and the models proposed by Leporini *et al.*[71–73] to experiments and simulations[24,75,76] emphasize that there are close interrelations between structural relaxation and vibrational dynamics for glass-forming liquids. These results also raise the question of the universality of α and the fundamental origin of this remarkable relation between the fast dynamics on a ps timescale and the structural relaxation occurring on a timescale on the order of minutes near the glass transition. We next

consider $<u^2>$ in relation to the mechanical properties (*e.g.*, shear modulus G and bulk modulus B) for our simulated thermoset material as the polymer stiffness parameter is varied.

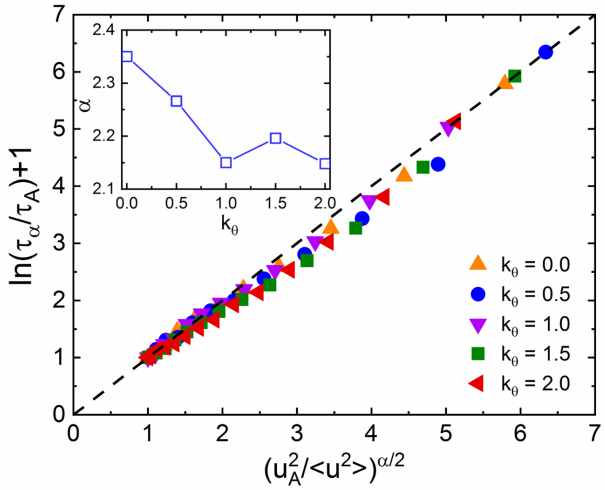

Figure 5. Tests of the localization model predictions (dashed line) for cross-linked polymer networks with varying chain stiffness k_θ. The data show a good collapse onto the localization model. The inset shows the estimated best fit values of the LM exponent α as a function of k_θ.

3.3. Mechanical Properties. The mechanical properties of cross-linked polymers play a vital role in the engineering and structural applications. The MC simulations on the semi-flexible polymer networks[77] and self-interacting wormlike chains[16] both indicated that increasing chain stiffness led to a higher elastic macroscopic modulus and a reduction in the extensibility of the material. Torres *et al.*[6] observed an important increase in the elastic modulus due to hindered torsional rotation when the chemical structure of polymer backbone changed from a monocyclic cyclopentyl to a bicyclic norbonyl ring. Crawford *et al.*[14] experimentally investigated the effect of chain stiffness on the mechanical properties of epoxy resins by altering the chemical structure of the amine groups of the epoxy, and they found that both the rubbery and glassy shear moduli were nearly independent of chain stiffness while the networks with aromatic moieties exhibited a

substantially higher compressive yield strength than the aliphatic resins. It is evidently difficult to discern any direct relation between molecular stiffness of the network chains and the macroscopic mechanical properties of thermoset materials. Of course, it is hard to explore the isolated effect of chain stiffness experimentally without changing the chemical nature of the polymers, which is one source of difficulty in seeking correlations between molecular parameters and mechanical properties.[7,22] In our previous work,[41,42] we observed a higher shear modulus and bulk modulus with the increasing cross-link density and cohesive energy for our cross-linked network models. Moreover, the mechanical properties collapsed onto a master curve when plotted at the reduced temperature T / T_g, demonstrating the important role of T_g in the elastic properties of our model thermoset materials, despite the kinetic nature of T_g.

As an extension of our previous studies,[41,42] we consider the variation of glassy shear modulus G for cross-linked networks having varying chain stiffness at fixed temperature and reduced temperature T / T_g, respectively. The glassy shear modulus is estimated from non-equilibrium molecular dynamics shear tests, which should be similar to real quenched polymer glasses in a non-equilibrium state. **Figure 6a** shows the variation of glassy shear modulus G at fixed temperature for cross-linked networks with a wide range of chain stiffness. In deeply glassy state, the shear modulus decreases with increasing chain stiffness. With the increasing temperature, the cross-linked networks with flexible chains have a lower T_g and first undergo the glass transition, along with an obvious decrease in shear modulus, while the rigid cross-linked networks are still in a glassy state with a slower decreasing trend in shear modulus. Thus, at near or above T_g (such as $T = 0.5\ \varepsilon / k_B$), the shear modulus becomes larger for cross-linked networks with rigid chains. Ness

et al.[7] systematically investigate the influence of bending constraints on the mechanical properties for linear polymer melts using CG-MD and non-affine lattice dynamics theory, where the bending energy ε_{bend} / ε_{LJ} ranges from 0.01 to 3000. They found that the storage modulus decreased first when the chains were relatively flexible and then progressively increased with the bending stiffness, and the minimum of storage modulus occurred at $2 < \varepsilon_{bend} / \varepsilon_{LJ} < 20$. They argued that the non-monotonic dependence of storage modulus was due to the competing effects of increasing chain stiffness and increasing "free volume". The range of bending energy in the work of Ness *et al.*[7] is much larger than our work, while the variation trends of moduli with the increasing bending energy are qualitatively consistent with those found in our work when the chain stiffness is relatively small. For the stiffer networks, such as nanocellulose network, this raises the question of how high chain stiffness influence the moduli of cross-linked networks. Thus, we emphasize here that the variation trends of shear modulus with the increasing chain stiffness is only limited in the coarse-grained models and the range of bending constraints used in the present work. **Figure 6b** further tests the variation of shear modulus at reduced temperature T / T_g. Opposed to the near universal data reduction observed in the fully flexible cross-linked networks with varying cross-link density and cohesive energy,[41,42] the glassy shear modulus decreases with the increasing chain stiffness, as found by Riggleman *et al.* in the linear polymer melts and their thin films.[49] Similarly, the storage modulus does not collapse onto a master curve at reduced temperature T / T_g in the linear polymer melts with varying chain bending stiffness, either.[7] Moreover, our bulk modulus B, estimated from the reciprocal of isothermal compressibility, similarly does not collapse onto a master curve (Figure S4 in the Supporting Information), and B tends to be smaller for stiffer chains

in the *T* range investigated. The different trends observed in the moduli of cross-linked networks with bending constraints emphasize the distinctive influence of varying chain stiffness on the mechanical properties of cross-linked thermosets.

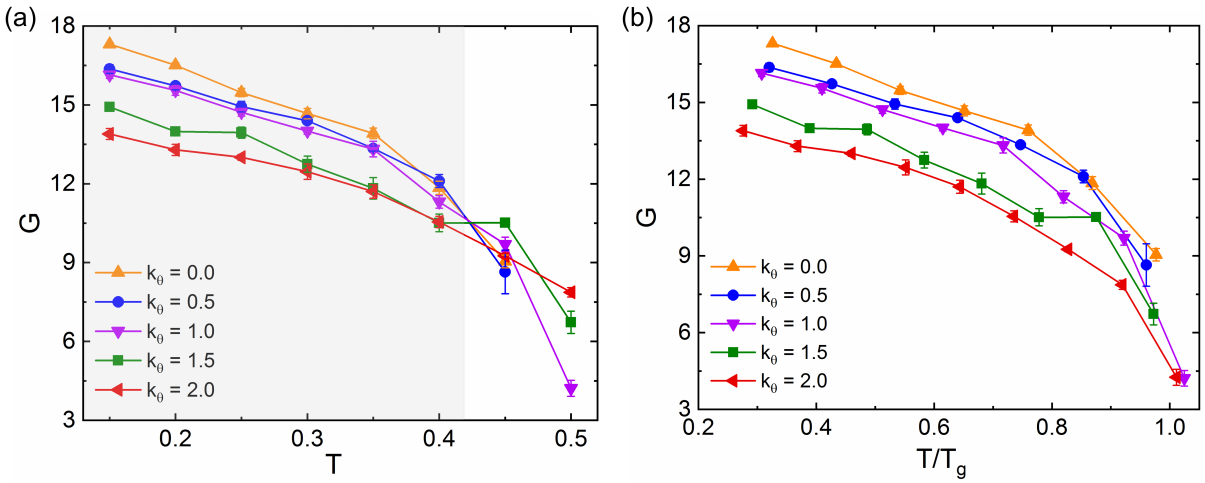

Figure 6. Glassy shear modulus *G* for cross-linked polymer networks with varying chain stiffness k_θ. (a) *G* at fixed temperature *T*. (b) *G* as a function of reduced temperature T / T_g.

It has been long recognized that there are scaling relationships among the structural relaxation time τ_α, glassy shear modulus *G* and Debye-Waller factor $\langle u^2 \rangle$ describing the mean square particle displacement on the timescale of the fast β-relaxation time. The Debye theory of solids held that the shear modulus *G* was proportional to $k_B T / \langle u^2 \rangle$ for a classic harmonic solid model.[78] However, this exact relationship failed for the glassy modulus of polymer materials, which presumably attributed to the highly anharmonic interactions found in liquids. To address this problem, Leporini and coworkers[71–73] have performed extensive MD simulations exploring the validity of this interesting relationship, which is not explained by any extent theory. Leporini *et al.*[72] first proposed a master curve to describe the relationship between $\langle u^2 \rangle$ and glassy elastic modulus, which was

confirmed in glass formers with a wide range of fragilities. This scaling relationship has been subsequently observed in a wide range of polymeric and metallic glass-forming materials, such as polycarbonate, nanocellulose networks, thin polymer films, and $Cu_{64}Zr_{36}$ metallic glass formers.[79–82] Here, we explore this scaling relationship for cross-linked networks with varying chain stiffness. The shear modulus G exhibits a linear relationship with the local stiffness $k_BT / \langle u^2 \rangle$ (**Figure 7a**), as observed in the fully flexible cross-linked networks with a wide range of cross-link densities and cohesive energy parameters.[41,42] Recently, Xu *et al.*[83] also observed this linear relationship in the linear polymer melts with variable pressure, chain stiffness and chain length, where the slope and intercept were material- and pressure-dependent. The simulations on the Zr-Cu metallic glass,[82] thin polymer films[81] and double-stranded DNA melts with varying bending stiffness[84] all indicated that the $k_BT / \langle u^2 \rangle$ could be taken as an "effective force constant" characterizing the "stiffness" of the bonds in a molecule. A physical interpretation on the empirical linear relationship between G and $k_BT / \langle u^2 \rangle$ was discussed by Zhang *et al.* for thin polymer films[81] and by Wang *et al.* based on the Cu-Zr metallic glass formers.[82]

Recently, Douglas and Xu[44] analyzed the scaling relationship between $\langle u^2 \rangle$ and the inverse of bulk modulus, isothermal compressibility κ_T based on the GET of a relation between the reduced configurational entropy, the configurational entropy normalized by its value at the onset temperature T_A, and a reduced isothermal compressibility. And they first proposed a function to describe the relationship between κ_T and $\langle u^2 \rangle$, $\kappa_T - \kappa_T^1 = \kappa_T^0 \times (\langle u^2 \rangle / u_A^2)^{3/2}$, which has successfully described the scaling relationship for linear polymer melts with variable chain stiffness and pressure. Later, we found that this proposed expression successfully described the scaling

relationship between the bulk modulus B and $\langle u^2 \rangle$ for fully flexible cross-linked thermosets with varying cross-link density and cohesive energy.[41,42] **Figure 7b** again confirms that the bulk modulus B indeed exhibits a near universal scaling relationship with $\langle u^2 \rangle$ for cross-linked networks with varying chain stiffness. In addition, we find the reciprocal of isothermal compressibility, B in our cross-linked networks with varying chain stiffness follows the function developed by Douglas and Xu[44] well (dashed curves in the **Figure 7b**), as observed in the cross-linked networks with varying cross-link density and fixed cohesive energy.[41,42] We notice, however, that the relationship between B and $\langle u^2 \rangle$ is different for T above or below T_g, which may well be a non-equilibrium effect. The specific fitting parameters are listed in the caption in **Figure 7b**. Recently, Jeong and Douglas[85] also successfully applied this type of scaling expression to an atomistic model of polyethylene and functionalized polyethylene. In addition, we emphasize that we are not aware of an experiment of either the predicted relation between G and $k_B T / \langle u^2 \rangle$ or the relation between B and $\langle u^2 \rangle$, but the applicability of these relations to simulation data seems to be robust. These scaling relationships should be further confirmed in the experiments for a wide range of glass-forming polymers. In general, $\langle u^2 \rangle$ exhibits an excellent scaling relationship with the moduli of cross-linked networks and linear polymer melts. These relationships have evident potential use in material design, given the relative ease of calculations of $\langle u^2 \rangle$.

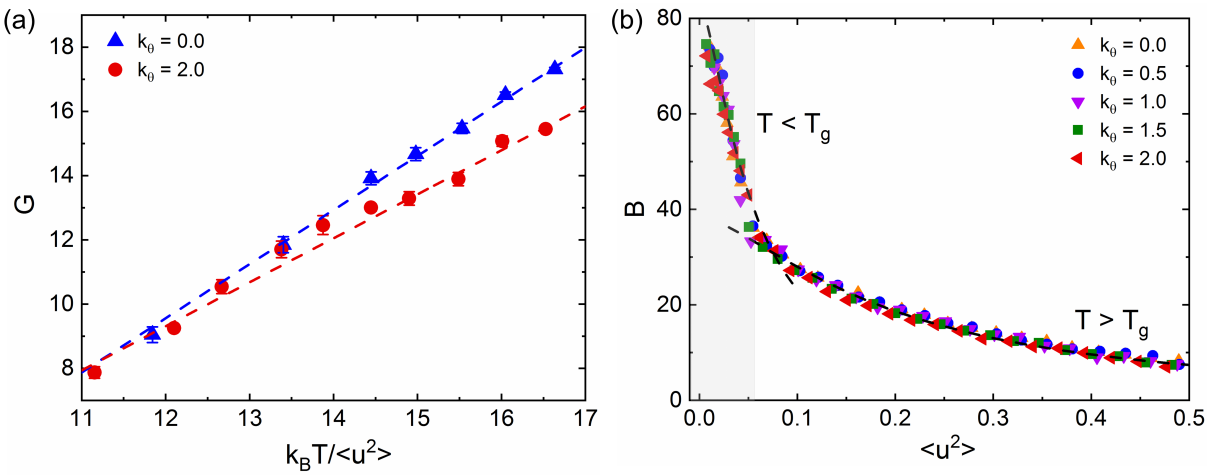

Figure 7. Relationship between moduli (shear modulus G and bulk modulus B) and Debye-Waller parameter $\langle u^2 \rangle$. (a) Shear modulus G as a function of local stiffness $k_BT / \langle u^2 \rangle$. The dashed lines descript the linear fitting, where G increases linearly with the $k_BT / \langle u^2 \rangle$. The error bars indicate the standard deviation of five shear tests. (b) Bulk modulus B as a function of $\langle u^2 \rangle$. The dashed curves are fitting lines with the function form $B = 1/\left[\kappa_T^0 \times (\langle u^2 \rangle / u_A^2)^{3/2} + \kappa_T^1\right]$, where $(\kappa_T^0,\ \kappa_T^1)$ are fitting parameters. The parameters $(\kappa_T^0/(u_A^2)^{3/2},\ \kappa_T^1)$ are (0.99, 0.012) for $T < T_g$ and (0.31, 0.026) for $T > T_g$. The coefficient of determination R^2 of fitting curves is 0.93 and 0.98, respectively.

3.4. Dynamical Heterogeneity. Elder *et al.*[31,39,40] performed a series of studies on dicyclopentadiene networks using the atomistic MD and experiments. They found that the mobility of atoms was significantly spatially heterogeneous, where the root-mean-square fluctuations of atomic positions indicated that the cross-links were less mobile than linear segments.[31] And the overall atomic mobility was progressively reduced with the increasing content of polar monomers, which was attributed to the increased cohesive energy density in the cross-linked networks.[39] The significant role of cohesive interaction strength played in the dynamical heterogeneity was also observed in our cross-linked networks over a wide range of cross-link densities.[42]

The effect of chain stiffness on the dynamical heterogeneity is estimated through the color map distribution of local stiffness $1 / \langle u^2 \rangle$ in **Figure 8**. The teal blue region indicates a small local molecular stiffness, and thus a relatively soft region, while the red domains correspond to stiff regions. **Figure 8a** shows the spatial distribution of local stiffness $1 / \langle u^2 \rangle$ at a higher fixed temperature, $T = 0.5\ \varepsilon / k_B$, where the shear modulus increases with the increasing chain stiffness. The variation of color in these maps corresponds to changes in local "stiffness" and variations of the relaxation time at higher T where these domains are transient. As the linear chains get stiffer, the color map changes from nearly teal blue to yellow-red dominated, which demonstrates that the overall rigidity of cross-linked network significantly increases. The color map values vary more sharply with increasing chain stiffness, indicating a greater degree of elastic heterogeneity. The color map of local stiffness is qualitatively consistent with previous observations in simulated polycarbonate glassy polymers with varying cohesive interaction strength,[79] nanocellulose networks with varying density and cohesive energy density,[80] and Zr-Cu metallic glasses.[82] **Figure 8b** further estimated the spatial distribution of local stiffness $1 / \langle u^2 \rangle$ at reduced temperature $T / T_g = 0.8$. The color maps turn from red to teal blue when the cross-linked polymer network gets stiffer, indicating a smaller local stiffness and a relatively softer material. The variation in the color map consists well with the decreasing trend in shear modulus with increasing chain stiffness in **Figure 6b**. In addition, when the chains get stiffer, the color variation becomes relatively mild, corresponding to a smaller degree of "dynamical heterogeneity".

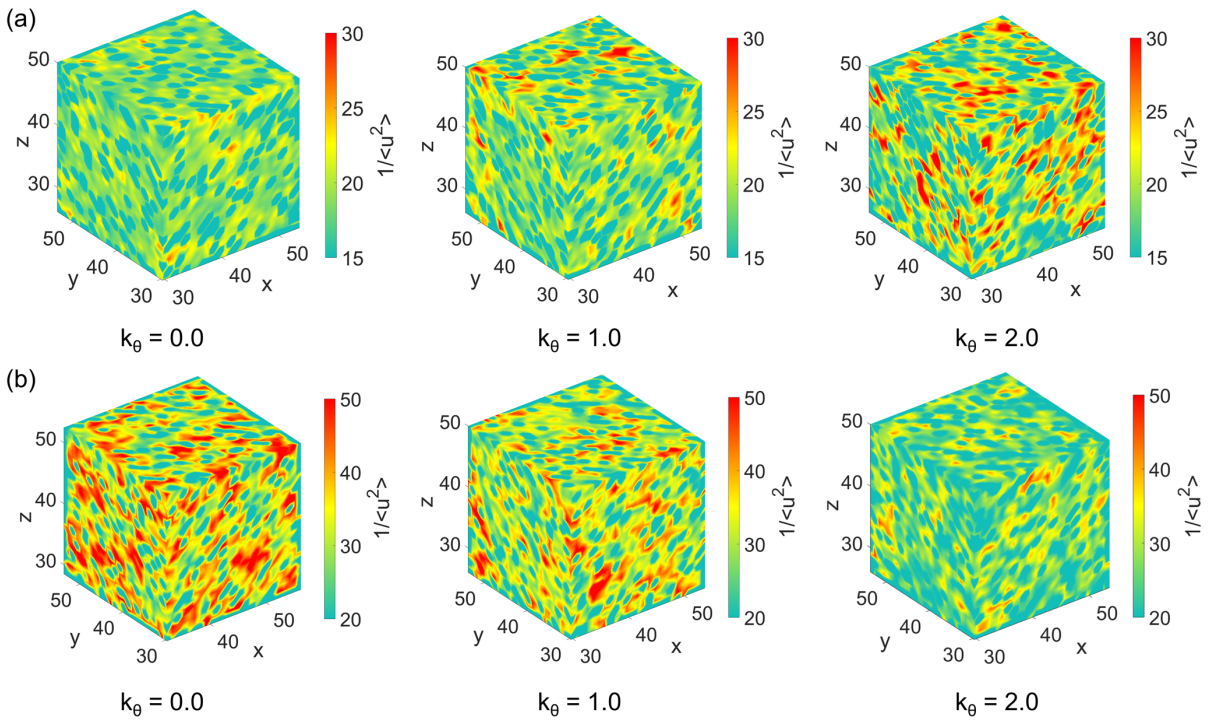

Figure 8. Color maps of local molecular stiffness $1 / \langle u^2 \rangle$ for cross-linked networks with varying chain stiffness k_θ. (a) At fixed temperature, $T = 0.5\ \varepsilon / k_B$. The color map scale is the same for all plots. (b) At reduced temperature $T / T_g = 0.8$. The color bar scale is the same for all plots.

To further assess the influence of chain stiffness on the elastic heterogeneity, we estimate the probability density distribution of the local stiffness $1 / \langle u^2 \rangle$ at fixed T and reduced temperature, respectively (**Figure 9**). We find that $P(1 / \langle u^2 \rangle)$ exhibits a nearly Gaussian form as observed in the fully flexible cross-linked networks,[41,42] where all the coefficients of determination of Gaussian distribution fitting are larger than 0.97. For clarity, only the Gaussian fitting curve is shown in **Figure 9**, and the original data can be found in the Figure S5 in the Supporting Information. We can see in **Figure 9a** that as the linear chains get stiffer, the peak position of local stiffness distribution becomes larger at fixed temperature $T = 0.5\ \varepsilon / k_B$, corresponding to a larger average molecular stiffness, a trend reported for shear modulus and color map above. The $P(1 / \langle u^2 \rangle)$

distribution becomes broader and the variance of local stiffness quantifying this trend becomes larger with increasing chain stiffness, indicating a greater degree of elastic heterogeneity. In addition, we find a smaller average local stiffness in cross-linked networks with stiffer chains at a reduced temperature T / T_g = 0.8 (**Figure 9b**). At the same time, the variance of $P(1 / \langle u^2 \rangle)$ decreases progressively with increasing chain stiffness, which indicates a slighter degree of elastic heterogeneity. In particular, $P(1 / \langle u^2 \rangle)$ was nearly universal at a fixed reduced temperature T / T_g in the case of fully flexible cross-linked networks with varying cross-link density and cohesive energy in our previous works.[41,42] The lack of a universal scaling of $P(1 / \langle u^2 \rangle)$ when chain stiffness is varied at a fixed reduced temperature T / T_g is consistent with the non-universality in the shear modulus as a function of T / T_g when chain stiffness is varied. We again find the qualitatively different effect of varying chain stiffness from varying the cohesive interaction strength and cross-link density in our model cross-linked polymers.

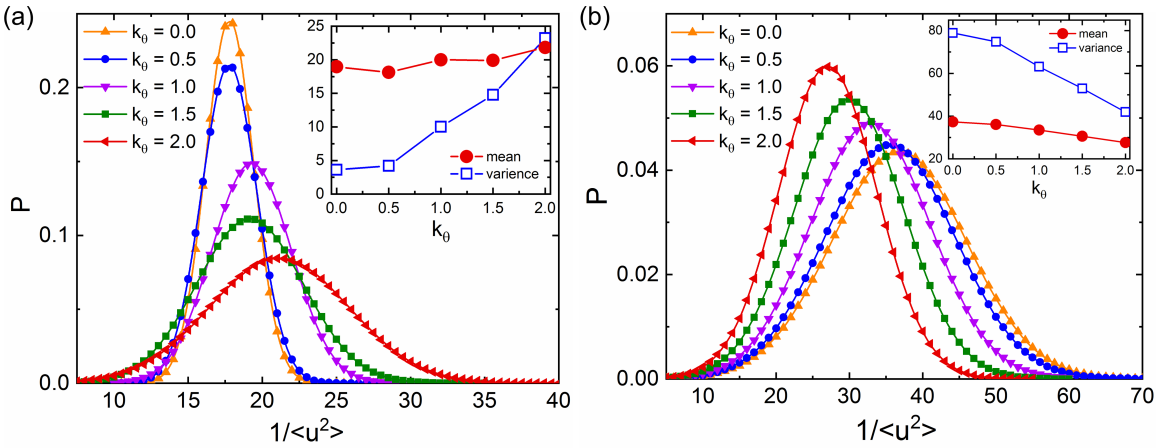

Figure 9. The probability density distribution, P, of local stiffness $1 / \langle u^2 \rangle$ for cross-linked networks with varying chain stiffness k_θ. The inset descripts the mean $1 / \langle u^2 \rangle$ and variance of the distribution of $P(1 / \langle u^2 \rangle)$ as a function of k_θ. (a) At fixed temperature $T = 0.5\ \varepsilon / k_B$. (b) At reduced temperature T / T_g = 0.8.

Another quantity commonly utilized to describe "dynamical heterogeneity" in glass-forming liquids is the non-Gaussian parameter, $\alpha_2(t) \equiv 3 \langle r^4(t) \rangle / (5 \langle r^2(t) \rangle^2) - 1$, where $r^2(t)$ is the mean-square displacement of a particle at time t from its initial position. $\alpha_2(t) = 0$ for Brownian motion, and thus $\alpha_2(t)$ specifically quantifies the deviation from Brownian diffusion symptomatic of the occurrence large mobility fluctuations in the cooled material.[43,50] Numerous studies on polymeric and metallic glass formers have repeatedly established that the peak position t^* of $\alpha_2(t)$ is related to the lifetime of mobile particle clusters, while the structural relaxation time τ_α corresponds to the lifetime of immobile particle clusters.[43,58,86] Our previous works found that there was a power-law relationship between t^* and τ_α in the fully flexible networks with varying cross-link density and cohesive energy.[41,42] We further quantify the effect of chain stiffness on the dynamical heterogeneity for our cross-linked network models.

We find that the amplitude and the peak position of $\alpha_2(t)$ both increase remarkably as the temperature decreases, corresponding to a greater degree of dynamical heterogeneity (**Figure 10a**). The similar trends were widely observed in glass-forming linear polymers with varying cohesive interaction strength[43] and chain stiffness,[50] star polymers with a wide range of star arms,[36] and cross-linked polymers with various cross-link densities.[5,41] Decreasing the temperature leads to not only a slower dynamics, but also a greater deviation of the particle displacement distribution from Gaussian form. In addition, it can be seen in **Figure 10a** that as T drops down to $T = 0.5\ \varepsilon / k_B$ (green curve), the amplitude of $\alpha_2(t)$ increases significantly from 0.5 to 2.2, providing a common measure of dynamical heterogeneity. The color maps and probability density distribution of local "stiffness" $k_B T / \langle u^2 \rangle$ (**Figure 8b** and **9b**) at a reduced temperature $T / T_g = 0.8$, which is somewhat

smaller than T_g for cross-linked thermosets, also exhibit evidence of obvious dynamic heterogeneity. **Figure 10b** estimates the relationship between the peak position of $\alpha_2(t)$, t^* and τ_α, where both t^* and τ_α are normalized by the fast β-relaxation time τ_f. A power-law scaling relationship, $t^* / \tau_f = A\ (\tau_\alpha / \tau_f)^{1-\zeta}$, is again observed where the exponent ζ is estimated to equal 0.29. A similar collapse was also observed in linear polymer melts with varying chain stiffness by Xu *et al.*,[46] while Pan *et al.*[50] found the power exponent slightly increased with chain stiffness. In addition, the exponent less than 1 indicates that there is a "decoupling" relationship between these timescales, consistent with previous observations in linear polymer melts,[43,46,50,86] and cross-linked networks having a wide range of cross-link densities and cohesive interaction strengths.[41,42] Recently, Zhang *et al.*[58] reported a similar decoupling between the normalized t^* / τ_f and τ_α / τ_f in Al-Sm metallic glasses, where the power-law exponent was found to be different at low and high temperatures. Starr *et al.*[86] systematically explored the particle motions in mobile and immobile clusters for linear glass-forming liquids. They found that the decoupling relation between t^* and τ_α matched well with the corresponding power-law relationship between the lifetimes of mobile particle clusters and immobile particle clusters.

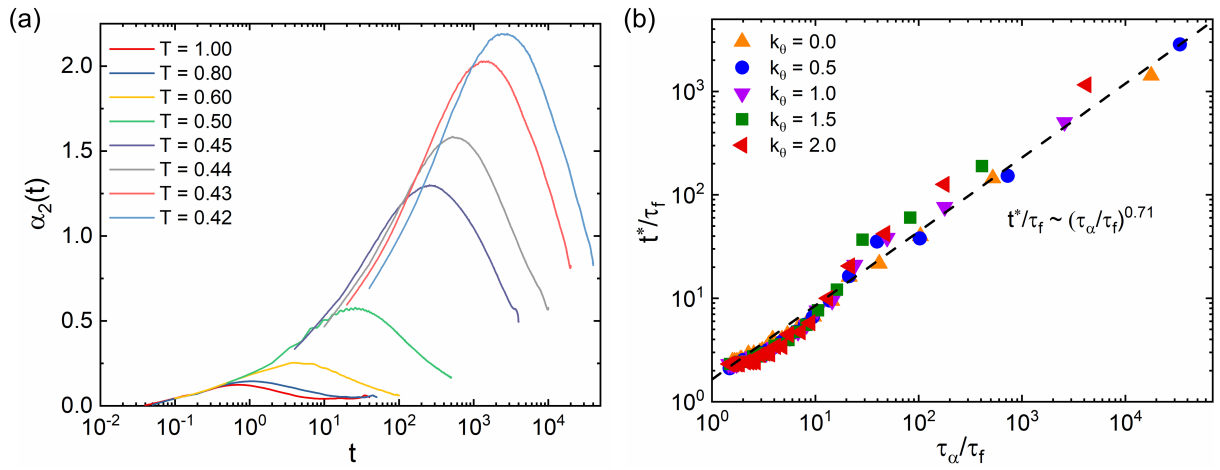

Figure 10. (a) Non-Gaussian parameter $\alpha_2(t)$ as a function of time t at different temperatures for cross-linked networks with chain stiffness k_θ = 0.0 ε. As T decreases, the amplitude and peak position of $\alpha_2(t)$ increase significantly. (b) The relationship between reduced non-Gaussian parameter peak time t^* / τ_f and reduced structural relaxation time τ_α / τ_f for various chain stiffness k_θ. Dashed line indicates the fit to a power-law relationship $t^* / \tau_f = A\ (\tau_\alpha / \tau_f)^{1-\zeta}$, where the fitting parameters (A, ζ) are determined to be (1.64, 0.29).

4. Conclusions

In the present work, we systematically investigated the influence of chain stiffness on the relaxation dynamics and mechanical properties of cross-linked polymer networks. We first explored the conformational properties, and found that the radius of gyration and persistence length both increased progressively with increasing chain stiffness for cross-linked polymer networks. This trend is not surprising, but this quantification of the stiffness variation of polymers is useful for making contact between experiments and simulations. The introduction of bending constraints led to significantly slower relaxation dynamics as expected, in company with an obvious increase in the characteristic temperatures (*e.g.*, onset temperature T_A, glass transition

temperature T_g, and Vogel temperature T_0) and fragility of glass formation K. By estimating the mechanical properties, we also observed that the shear modulus decreased with the increasing chain stiffness at a fixed reduced temperature T / T_g. Notably, the moduli G and B did not follow a near universal scaling with the reduced temperature as that found in previous simulations of ideally flexible chain networks with varying cross-linked density and cohesive interaction strength, which emphasizes the important role of bending constraints played in the mechanical properties of cross-linked network materials. Historically, it has been difficult to discern any direct relation between stiffness of the network chains and the macroscopic mechanical properties of thermoset materials, because it is generally difficult to explore the isolated effect of chain stiffness in real network materials without changing the chemical nature of polymers. This is obvious a source of difficulty in seeking correlations between molecular parameters and mechanical properties.

Despite these unexpected trends in G and B when the chain stiffness was varied, the structural relaxation time τ_α, G and B of the cross-linked semi-flexible networks exhibited a convincing and general scaling relationships with the Debye-Waller parameter $\langle u^2 \rangle$, a quantity also utilized to estimate the local stiffness fluctuations of our model thermoset materials. By quantifying the spatial distribution and probability density distribution of local stiffness parameter, $1 / \langle u^2 \rangle$, we found that the "elastic heterogeneity" (a measure of dynamical heterogeneity) decreased as the chains became stiffer at the same reduced temperature T / T_g. The findings of the present work reveal the unique impact of varying chain stiffness on the segmental relaxation dynamics and mechanical properties of cross-linked networks. The driving hypothesis underlying the present work is that a more fundamental understanding of how the dynamical properties of polymer

network materials depend on molecular parameters should enable the more rational design of thermoset materials, and other polymer network materials of interest, including “vitrimers” and telechelics in which the cross-links are of a physical nature. The present work demonstrates the advantageous use of coarse-grained models for identifying general trends in dynamical and mechanical properties of this broad class of materials, because the numerous molecular parameters describing most any real material from an atomistic standpoint have been reduced to a minimal set of variables describing chain flexibility, cohesive interaction strength, and cross-link density.

Associated Content

Supporting Information

Thermodynamical properties (Figure S1), fast β-relaxation dynamics (Figure S2), the relaxation dynamics for uncross-linked melts (Figure S3), bulk modulus as a function of reduced temperature T / T_g (Figure S4) and probability density distribution of local stiffness 1 / $\langle u^2 \rangle$ (Figure S5).

Acknowledgements

X.Z. and Y.G. acknowledge the support from the National Natural Science Foundation of China (Grant No.12172038). W.X. and W.N. acknowledges the support from the U.S. Office of Naval Research (Award No. N00014-22-1-2129) and Department of Aerospace Engineering at Iowa State University. J.F.D acknowledges the support from the National Institute of Standards and Technology.

References

(1) Napolitano, S.; Glynos, E.; Tito, N. B. Glass Transition of Polymers in Bulk, Confined Geometries, and near Interfaces. *Rep. Prog. Phys.* **2017**, *80* (3), 036602. https://doi.org/10.1088/1361-6633/aa5284.

(2) Kunal, K.; Robertson, C. G.; Pawlus, S.; Hahn, S. F.; Sokolov, A. P. Role of Chemical Structure in Fragility of Polymers: A Qualitative Picture. *Macromolecules* **2008**, *41* (19), 7232–7238. https://doi.org/10.1021/ma801155c.

(3) Duarte, D. M.; Tu, W.; Dzienia, A.; Adrjanowicz, K. Study on the Effect of Side-Chain Group on the Segmental Dynamics of Selected Methacrylate Polymers at Ambient and High Pressures. *Polymer* **2019**, *183*, 121860. https://doi.org/10.1016/j.polymer.2019.121860.

(4) Casalini, R.; Roland, C. M. Effect of Crosslinking on the Secondary Relaxation in Polyvinylethylene. *J. Polym. Sci. Part B Polym. Phys.* **2010**, *48* (5), 582–587. https://doi.org/10.1002/polb.21925.

(5) Jia, X.-M.; Lin, W.-F.; Zhao, H.-Y.; Qian, H.-J.; Lu, Z.-Y. Supercooled Melt Structure and Dynamics of Single-Chain Nanoparticles: A Computer Simulation Study. *J. Chem. Phys.* **2021**, *155* (5), 054901. https://doi.org/10.1063/5.0056293.

(6) Torres, J. M.; Wang, C.; Coughlin, E. B.; Bishop, J. P.; Register, R. A.; Riggleman, R. A.; Stafford, C. M.; Vogt, B. D. Influence of Chain Stiffness on Thermal and Mechanical Properties of Polymer Thin Films. *Macromolecules* **2011**, *44* (22), 9040–9045.

https://doi.org/10.1021/ma201482b.

(7) Ness, C.; Palyulin, V. V.; Milkus, R.; Elder, R.; Sirk, T.; Zaccone, A. Nonmonotonic Dependence of Polymer-Glass Mechanical Response on Chain Bending Stiffness. *Phys. Rev. E* **2017**, *96* (3), 030501(R). https://doi.org/10.1103/PhysRevE.96.030501.

(8) Rana, D.; Sauvant, V.; Halary, J. L. Molecular Analysis of Yielding in Pure and Antiplasticized Epoxy-Amine Thermosets. *J. Mater. Sci.* **2002**, *37* (24), 5267–5274. https://doi.org/10.1023/A:1021012721619.

(9) McKenzie-Smith, T. Q.; Douglas, J. F.; Starr, F. W. Explaining the Sensitivity of Polymer Segmental Relaxation to Additive Size Based on the Localization Model. *Phys. Rev. Lett.* **2021**, *127* (27), 277802. https://doi.org/10.1103/PhysRevLett.127.277802.

(10) Ngai, K. L.; Roland, C. M. Chemical Structure and Intermolecular Cooperativity: Dielectric Relaxation Results. *Macromolecules* **1993**, *26* (25), 6824–6830. https://doi.org/10.1021/ma00077a019.

(11) Agapov, A. L.; Sokolov, A. P. Decoupling Ionic Conductivity from Structural Relaxation: A Way to Solid Polymer Electrolytes? *Macromolecules* **2011**, *44* (11), 4410–4414. https://doi.org/10.1021/ma2001096.

(12) Wang, Y.; Agapov, A. L.; Fan, F.; Hong, K.; Yu, X.; Mays, J.; Sokolov, A. P. Decoupling of Ionic Transport from Segmental Relaxation in Polymer Electrolytes. *Phys. Rev. Lett.* **2012**, *108* (8), 088303. https://doi.org/10.1103/PhysRevLett.108.088303.

(13) Kumar, R.; Goswami, M.; Sumpter, B. G.; Novikov, V. N.; Sokolov, A. P. Effects of Backbone Rigidity on the Local Structure and Dynamics in Polymer Melts and Glasses.

Phys. Chem. Chem. Phys. **2013**, *15* (13), 4604–4609. https://doi.org/10.1039/c3cp43737j.

(14) Crawford, E.; Lesser, A. J. The Effect of Network Architecture on the Thermal and Mechanical Behavior of Epoxy Resins. *J. Polym. Sci. Part B Polym. Phys.* **1998**, *36* (8), 1371–1382. https://doi.org/10.1002/(SICI)1099-0488(199806)36:8<1371::AID-POLB11>3.0.CO;2-4.

(15) Lesser, A. J.; Calzia, K. J. Molecular Parameters Governing the Yield Response of Epoxy-Based Glassy Networks. *J. Polym. Sci. Part B Polym. Phys.* **2004**, *42* (11), 2050–2056. https://doi.org/10.1002/polb.20090.

(16) Cifra, P.; Bleha, T. Stretching of Self-Interacting Wormlike Macromolecules. *Polymer* **2007**, *48* (8), 2444–2452. https://doi.org/10.1016/j.polymer.2007.02.031.

(17) Cifra, P.; Bleha, T. Free Energy of Deformation of the Radius of Gyration in Semiflexible Chains. *Macromol. Theory Simulations* **2007**, *16* (5), 501–512. https://doi.org/10.1002/mats.200700023.

(18) Narambuena, C. F.; Leiva, E. P. M.; Chávez-Páez, M.; Pérez, E. Effect of Chain Stiffness on the Morphology of Polyelectrolyte Complexes. A Monte Carlo Simulation Study. *Polymer* **2010**, *51* (14), 3293–3302. https://doi.org/10.1016/j.polymer.2010.04.065.

(19) Huang, J.-H.; Sun, D.-D.; Lu, R.-X. Glass Transition and Dynamics of Semiflexible Polymer Brushes. *Phys. Chem. Chem. Phys.* **2021**, *23* (25), 13895–13904. https://doi.org/10.1039/D1CP00089F.

(20) Ruan, D.; Simmons, D. S. Roles of Chain Stiffness and Segmental Rattling in Ionomer Glass Formation. *J. Polym. Sci. Part B Polym. Phys.* **2015**, *53* (20), 1458–1469.

https://doi.org/10.1002/polb.23788.

(21) Xie, S.-J.; Qian, H.-J.; Lu, Z.-Y. The Glass Transition of Polymers with Different Side-Chain Stiffness Confined in Free-Standing Thin Films. *J. Chem. Phys.* **2015**, *142* (7), 074902. https://doi.org/10.1063/1.4908047.

(22) Peng, Y.; Zhang, H.; Huang, X.-W.; Huang, J.-H.; Luo, M.-B. Monte Carlo Simulation on the Dynamics of a Semi-Flexible Polymer in the Presence of Nanoparticles. *Phys. Chem. Chem. Phys.* **2018**, *20* (41), 26333–26343. https://doi.org/10.1039/C8CP05136D.

(23) Xu, W.-S.; Freed, K. F. Influence of Cohesive Energy and Chain Stiffness on Polymer Glass Formation. *Macromolecules* **2014**, *47* (19), 6990–6997. https://doi.org/10.1021/ma501581u.

(24) Mangalara, J. H.; Simmons, D. S. Tuning Polymer Glass Formation Behavior and Mechanical Properties with Oligomeric Diluents of Varying Stiffness. *ACS Macro Lett.* **2015**, *4* (10), 1134–1138. https://doi.org/10.1021/acsmacrolett.5b00635.

(25) Xu, X.; Douglas, J. F.; Xu, W.-S. Influence of Side-Chain Length and Relative Rigidities of Backbone and Side Chains on Glass Formation of Branched Polymers. *Macromolecules* **2021**, *54* (13), 6327–6341. https://doi.org/10.1021/acs.macromol.1c00834.

(26) Dudowicz, J.; Freed, K. F.; Douglas, J. F. Generalized Entropy Theory of Polymer Glass Formation. *Adv. Chem. Phys.* **2008**, *137*, 125–222. https://doi.org/10.1002/9780470238080.ch3.

(27) Casalini, R.; Corezzi, S.; Fioretto, D.; Livi, A.; Rolla, P. A. Unified Dielectric Description of the Dynamics of Polymeric Systems Undergoing Either Thermal or Chemical

Vitrification. *Chem. Phys. Lett.* **1996**, *258* (3–4), 470–476. https://doi.org/10.1016/0009-2614(96)00654-9.

(28) Corezzi, S.; Fioretto, D.; Rolla, P. Bond-Controlled Configurational Entropy Reduction in Chemical Vitrification. *Nature* **2002**, *420* (6916), 653–656. https://doi.org/10.1038/nature01261.

(29) Beiner, M.; Ngai, K. L. Interrelation between Primary and Secondary Relaxations in Polymerizing Systems Based on Epoxy Resins. *Macromolecules* **2005**, *38* (16), 7033–7042. https://doi.org/10.1021/ma050384j.

(30) Mei, B.; Lin, T.-W.; Sheridan, G. S.; Evans, C. M.; Sing, C. E.; Schweizer, K. S. Structural Relaxation and Vitrification in Dense Cross-Linked Polymer Networks: Simulation, Theory, and Experiment. *Macromolecules* **2022**, *55* (10), 4159–4173. https://doi.org/10.1021/acs.macromol.2c00277.

(31) Elder, R. M.; Andzelm, J. W.; Sirk, T. W. A Molecular Simulation Study of the Glass Transition of Cross-Linked Poly(Dicyclopentadiene) Networks. *Chem. Phys. Lett.* **2015**, *637*, 103–109. https://doi.org/10.1016/j.cplett.2015.07.058.

(32) Alves, N. M.; Gómez Ribelles, J. L.; Mano, J. F. Enthalpy Relaxation Studies in Polymethyl Methacrylate Networks with Different Crosslinking Degrees. *Polymer* **2005**, *46* (2), 491–504. https://doi.org/10.1016/j.polymer.2004.11.016.

(33) Vargas-Lara, F.; Pazmiño Betancourt, B. A.; Douglas, J. F. Influence of Knot Complexity on Glass-Formation in Low Molecular Mass Ring Polymer Melts. *J. Chem. Phys.* **2019**, *150* (10), 101103. https://doi.org/10.1063/1.5085425.

(34) Vargas-Lara, F.; Pazmiño Betancourt, B. A.; Douglas, J. F. Communication: A Comparison between the Solution Properties of Knotted Ring and Star Polymers. *J. Chem. Phys.* **2018**, *149* (16), 161101. https://doi.org/10.1063/1.5048937.

(35) Zhang, W.; Douglas, J. F.; Chremos, A.; Starr, F. W. Structure and Dynamics of Star Polymer Films from Coarse-Grained Molecular Simulations. *Macromolecules* **2021**, *54* (12), 5344–5353. https://doi.org/10.1021/acs.macromol.1c00504.

(36) Fan, J.; Emamy, H.; Chremos, A.; Douglas, J. F.; Starr, F. W. Dynamic Heterogeneity and Collective Motion in Star Polymer Melts. *J. Chem. Phys.* **2020**, *152* (5), 054904. https://doi.org/10.1063/1.5135731.

(37) Chremos, A.; Douglas, J. F. Communication: When Does a Branched Polymer Become a Particle? *J. Chem. Phys.* **2015**, *143* (11), 111104. https://doi.org/10.1063/1.4931483.

(38) Chremos, A.; Douglas, J. F. A Comparative Study of Thermodynamic, Conformational, and Structural Properties of Bottlebrush with Star and Ring Polymer Melts. *J. Chem. Phys.* **2018**, *149* (4), 044904. https://doi.org/10.1063/1.5034794.

(39) Elder, R. M.; Long, T. R.; Bain, E. D.; Lenhart, J. L.; Sirk, T. W. Mechanics and Nanovoid Nucleation Dynamics: Effects of Polar Functionality in Glassy Polymer Networks. *Soft Matter* **2018**, *14* (44), 8895–8911. https://doi.org/10.1039/C8SM01483C.

(40) Elder, R. M.; Forster, A. L.; Krishnamurthy, A.; Dennis, J. M.; Akiba, H.; Yamamuro, O.; Ito, K.; Evans, K. M.; Soles, C.; Sirk, T. W. Relative Effects of Polymer Composition and Sample Preparation on Glass Dynamics. *Soft Matter* **2022**, *18* (35), 6511–6516. https://doi.org/10.1039/D2SM00698G.

(41) Zheng, X.; Guo, Y.; Douglas, J. F.; Xia, W. Understanding the Role of Cross-Link Density in the Segmental Dynamics and Elastic Properties of Cross-Linked Thermosets. *J. Chem. Phys.* **2022**, *157* (6), 064901. https://doi.org/10.1063/5.0099322.

(42) Zheng, X.; Guo, Y.; Douglas, J. F.; Xia, W. Competing Effects of Cohesive Energy and Cross-Link Density on the Segmental Dynamics and Mechanical Properties of Cross-Linked Polymers. *Macromolecules* **2022**, *55* (22), 9990–10004. https://doi.org/10.1021/acs.macromol.2c01719.

(43) Xu, W.-S.; Douglas, J. F.; Freed, K. F. Influence of Cohesive Energy on Relaxation in a Model Glass-Forming Polymer Melt. *Macromolecules* **2016**, *49* (21), 8355–8370. https://doi.org/10.1021/acs.macromol.6b01504.

(44) Douglas, J. F.; Xu, W.-S. Equation of State and Entropy Theory Approach to Thermodynamic Scaling in Polymeric Glass-Forming Liquids. *Macromolecules* **2021**, *54* (7), 3247–3269. https://doi.org/10.1021/acs.macromol.1c00075.

(45) Xu, W.-S.; Douglas, J. F.; Sun, Z.-Y. Polymer Glass Formation: Role of Activation Free Energy, Configurational Entropy, and Collective Motion. *Macromolecules* **2021**, *54* (7), 3001–3033. https://doi.org/10.1021/acs.macromol.0c02740.

(46) Xu, W.-S.; Douglas, J. F.; Xu, X. Molecular Dynamics Study of Glass Formation in Polymer Melts with Varying Chain Stiffness. *Macromolecules* **2020**, *53* (12), 4796–4809. https://doi.org/10.1021/acs.macromol.0c00731.

(47) Xu, W.-S.; Douglas, J. F.; Xu, X. Role of Cohesive Energy in Glass Formation of Polymers with and without Bending Constraints. *Macromolecules* **2020**, *53* (22), 9678–

9697. https://doi.org/10.1021/acs.macromol.0c01876.

(48) Kremer, K.; Grest, G. S. Dynamics of Entangled Linear Polymer Melts: A Molecular-Dynamics Simulation. *J. Chem. Phys.* **1990**, *92* (8), 5057–5086. https://doi.org/10.1063/1.458541.

(49) Shavit, A.; Riggleman, R. A. Influence of Backbone Rigidity on Nanoscale Confinement Effects in Model Glass-Forming Polymers. *Macromolecules* **2013**, *46* (12), 5044–5052. https://doi.org/10.1021/ma400210w.

(50) Pan, D.; Sun, Z.-Y. Influence of Chain Stiffness on the Dynamical Heterogeneity and Fragility of Polymer Melts. *J. Chem. Phys.* **2018**, *149* (23), 234904. https://doi.org/10.1063/1.5052153.

(51) Everaers, R.; Karimi-Varzaneh, H. A.; Fleck, F.; Hojdis, N.; Svaneborg, C. Kremer–Grest Models for Commodity Polymer Melts: Linking Theory, Experiment, and Simulation at the Kuhn Scale. *Macromolecules* **2020**, *53* (6), 1901–1916. https://doi.org/10.1021/acs.macromol.9b02428.

(52) Thompson, A. P.; Metin Aktulga, H.; Berger, R.; Bolintineanu, D. S.; Michael Brown, W.; Crozier, P. S.; in ’t Veld, P. J.; Kohlmeyer, A.; Moore, S. G.; Nguyen, T. D.; Shan, R.; Stevens, M. J.; Tranchida, J.; Trott, C.; Plimpton, S. J. LAMMPS - a Flexible Simulation Tool for Particle-Based Materials Modeling at the Atomic, Meso, and Continuum Scales. *Comput. Phys. Commun.* **2022**, *271*, 108171. https://doi.org/10.1016/j.cpc.2021.108171.

(53) Varshney, V.; Patnaik, S. S.; Roy, A. K.; Farmer, B. L. A Molecular Dynamics Study of Epoxy-Based Networks: Cross-Linking Procedure and Prediction of Molecular and

Material Properties. *Macromolecules* **2008**, *41* (18), 6837–6842. https://doi.org/10.1021/ma801153e.

(54) Bandyopadhyay, A.; Valavala, P. K.; Clancy, T. C.; Wise, K. E.; Odegard, G. M. Molecular Modeling of Crosslinked Epoxy Polymers: The Effect of Crosslink Density on Thermomechanical Properties. *Polymer* **2011**, *52* (11), 2445–2452. https://doi.org/10.1016/j.polymer.2011.03.052.

(55) Shokuhfar, A.; Arab, B. The Effect of Cross Linking Density on the Mechanical Properties and Structure of the Epoxy Polymers: Molecular Dynamics Simulation. *J. Mol. Model.* **2013**, *19* (9), 3719–3731. https://doi.org/10.1007/s00894-013-1906-9.

(56) Chen, W.; Chen, J.; Liu, L.; Xu, X.; An, L. Effects of Chain Stiffness on Conformational and Dynamical Properties of Individual Ring Polymers in Shear Flow. *Macromolecules* **2013**, *46* (18), 7542–7549. https://doi.org/10.1021/ma401137c.

(57) Xia, W.; Song, J.; Hsu, D. D.; Keten, S. Side-Group Size Effects on Interfaces and Glass Formation in Supported Polymer Thin Films. *J. Chem. Phys.* **2017**, *146* (20), 203311. https://doi.org/10.1063/1.4976702.

(58) Zhang, H.; Wang, X.; Yu, H.-B.; Douglas, J. F. Dynamic Heterogeneity, Cooperative Motion, and Johari–Goldstein β-Relaxation in a Metallic Glass-Forming Material Exhibiting a Fragile-to-Strong Transition. *Eur. Phys. J. E* **2021**, *44* (4), 56. https://doi.org/10.1140/epje/s10189-021-00060-7.

(59) Giuntoli, A.; Puosi, F.; Leporini, D.; Starr, F. W.; Douglas, J. F. Predictive Relation for the α-Relaxation Time of a Coarse-Grained Polymer Melt under Steady Shear. *Sci. Adv.*

2020, *6* (17), eaaz0777. https://doi.org/10.1126/sciadv.aaz0777.

(60) Zhang, H.; Wang, X.; Yu, H.-B.; Douglas, J. F. Fast Dynamics in a Model Metallic Glass-Forming Material. *J. Chem. Phys.* **2021**, *154* (8), 084505. https://doi.org/10.1063/5.0039162.

(61) Wang, Y.; Li, Z.; Niu, K.; Xia, W. Energy Renormalization for Coarse-Graining of Thermomechanical Behaviors of Conjugated Polymer. *Polymer* **2022**, *256*, 125159. https://doi.org/10.1016/j.polymer.2022.125159.

(62) Dudowicz, J.; Freed, K. F.; Douglas, J. F. Direct Computation of Characteristic Temperatures and Relaxation Times for Glass-Forming Polymer Liquids. *J. Chem. Phys.* **2005**, *123* (11), 111102. https://doi.org/10.1063/1.2035087.

(63) Freed, K. F. Influence of Monomer Molecular Structure on the Glass Transition in Polymers I. Lattice Cluster Theory for the Configurational Entropy. *J. Chem. Phys.* **2003**, *119* (11), 5730–5739. https://doi.org/10.1063/1.1600716.

(64) Adam, G.; Gibbs, J. H. On the Temperature Dependence of Cooperative Relaxation Properties in Glass-Forming Liquids. *J. Chem. Phys.* **1965**, *43* (1), 139–146. https://doi.org/10.1063/1.1696442.

(65) Mangalara, J. H.; Marvin, M. D.; Wiener, N. R.; Mackura, M. E.; Simmons, D. S. Does Fragility of Glass Formation Determine the Strength of T_g-Nanoconfinement Effects? *J. Chem. Phys.* **2017**, *146* (10), 104902. https://doi.org/10.1063/1.4976521.

(66) Stukalin, E. B.; Douglas, J. F.; Freed, K. F. Application of the Entropy Theory of Glass Formation to Poly(α-Olefins). *J. Chem. Phys.* **2009**, *131* (11), 114905.

https://doi.org/10.1063/1.3216109.

(67) Starr, F. W.; Douglas, J. F. Modifying Fragility and Collective Motion in Polymer Melts with Nanoparticles. *Phys. Rev. Lett.* **2011**, *106* (11), 115702. https://doi.org/10.1103/PhysRevLett.106.115702.

(68) Dudowicz, J.; Douglas, J. F.; Freed, K. F. The Meaning of the "Universal" WLF Parameters of Glass-Forming Polymer Liquids. *J. Chem. Phys.* **2015**, *142* (1), 014905. https://doi.org/10.1063/1.4905216.

(69) Kannurpatti, A. R.; Bowman, C. N. Structural Evolution of Dimethacrylate Networks Studied by Dielectric Spectroscopy. *Macromolecules* **1998**, *31* (10), 3311–3316. https://doi.org/10.1021/ma970721r.

(70) Starr, F. W.; Sastry, S.; Douglas, J. F.; Glotzer, S. C. What Do We Learn from the Local Geometry of Glass-Forming Liquids? *Phys. Rev. Lett.* **2002**, *89* (12), 125501. https://doi.org/10.1103/PhysRevLett.89.125501.

(71) Larini, L.; Ottochian, A.; De Michele, C.; Leporini, D. Universal Scaling between Structural Relaxation and Vibrational Dynamics in Glass-Forming Liquids and Polymers. *Nat. Phys.* **2008**, *4* (1), 42–45. https://doi.org/10.1038/nphys788.

(72) Puosi, F.; Leporini, D. The Kinetic Fragility of Liquids as Manifestation of the Elastic Softening. *Eur. Phys. J. E* **2015**, *38* (8), 87. https://doi.org/10.1140/epje/i2015-15087-2.

(73) Puosi, F.; Leporini, D. Communication: Correlation of the Instantaneous and the Intermediate-Time Elasticity with the Structural Relaxation in Glassforming Systems. *J. Chem. Phys.* **2012**, *136* (4), 041104. https://doi.org/10.1063/1.3681291.

(74) Simmons, D. S.; Cicerone, M. T.; Zhong, Q.; Tyagi, M.; Douglas, J. F. Generalized Localization Model of Relaxation in Glass-Forming Liquids. *Soft Matter* **2012**, *8* (45), 11455–11461. https://doi.org/10.1039/c2sm26694f.

(75) Pazmiño Betancourt, B. A.; Hanakata, P. Z.; Starr, F. W.; Douglas, J. F. Quantitative Relations between Cooperative Motion, Emergent Elasticity, and Free Volume in Model Glass-Forming Polymer Materials. *Proc. Natl. Acad. Sci.* **2015**, *112* (10), 2966–2971. https://doi.org/10.1073/pnas.1418654112.

(76) Hung, J.-H.; Patra, T. K.; Meenakshisundaram, V.; Mangalara, J. H.; Simmons, D. S. Universal Localization Transition Accompanying Glass Formation: Insights from Efficient Molecular Dynamics Simulations of Diverse Supercooled Liquids. *Soft Matter* **2019**, *15* (6), 1223–1242. https://doi.org/10.1039/C8SM02051E.

(77) Bhawe, D. M.; Cohen, C.; Escobedo, F. A. Formation and Characterization of Semiflexible Polymer Networks via Monte Carlo Simulations. *Macromolecules* **2004**, *37* (10), 3924–3933. https://doi.org/10.1021/ma0354896.

(78) Buchenau, U.; Zorn, R.; Ramos, M. A. Probing Cooperative Liquid Dynamics with the Mean Square Displacement. *Phys. Rev. E* **2014**, *90* (4), 042312. https://doi.org/10.1103/PhysRevE.90.042312.

(79) Alesadi, A.; Xia, W. Understanding the Role of Cohesive Interaction in Mechanical Behavior of a Glassy Polymer. *Macromolecules* **2020**, *53* (7), 2754–2763. https://doi.org/10.1021/acs.macromol.0c00067.

(80) Li, Z.; Xia, W. Coarse-Grained Modeling of Nanocellulose Network towards

Understanding the Mechanical Performance. *Extrem. Mech. Lett.* **2020**, *40*, 100942. https://doi.org/10.1016/j.eml.2020.100942.

(81) Zhang, W.; Starr, F. W.; Douglas, J. F. Activation Free Energy Gradient Controls Interfacial Mobility Gradient in Thin Polymer Films. *J. Chem. Phys.* **2021**, *155* (17), 174901. https://doi.org/10.1063/5.0064866.

(82) Wang, X.; Zhang, H.; Douglas, J. F. The Initiation of Shear Band Formation in Deformed Metallic Glasses from Soft Localized Domains. *J. Chem. Phys.* **2021**, *155* (20), 204504. https://doi.org/10.1063/5.0069729.

(83) Xu, X.; Douglas, J. F.; Xu, W.-S. Parallel Emergence of Rigidity and Collective Motion in a Family of Simulated Glass-Forming Polymer Fluids. *Macromolecules* **2023**, *56* (13), 4929–4951. https://doi.org/10.1021/acs.macromol.3c00184.

(84) Vargas-Lara, F.; Starr, F. W.; Douglas, J. F. Molecular Rigidity and Enthalpy–Entropy Compensation in DNA Melting. *Soft Matter* **2017**, *13* (44), 8309–8330. https://doi.org/10.1039/C7SM01220A.

(85) Jeong, C.; Starr, F. W.; Beers, K. L.; Douglas, J. F. Influence of Functionalization on the Crystallinity and Basic Thermodynamic Properties of Polyethylene. *Macromolecules* **2023**, *56* (11), 3873–3883. https://doi.org/10.1021/acs.macromol.2c02569.

(86) Starr, F. W.; Douglas, J. F.; Sastry, S. The Relationship of Dynamical Heterogeneity to the Adam-Gibbs and Random First-Order Transition Theories of Glass Formation. *J. Chem. Phys.* **2013**, *138* (12), 12A541. https://doi.org/10.1063/1.4790138.

Table of Content Figure